Charge fluctuations in open chaotic cavities

2005 J. Phys. A: Math. Gen. 38 10559

(http://iopscience.iop.org/0305-4470/38/49/008)

INSTITUTE OF PHYSICS PUBLISHING JOURNAL OF PHYSICS A: MATHEMATICAL AND GENERAL

J. Phys. A: Math. Gen. **38** (2005) 10559–10585 doi:10.1088/0305-4470/38/49/008

Charge fluctuations in open chaotic cavities

M Büttiker and M L Polianski

Département de Physique Théorique, Université de Genève, CH-1211 Genève 4, Switzerland

Received 8 August 2005
Published 22 November 2005
Online at stacks.iop.org/JPhysA/38/10559

Abstract

We present a discussion of the charge response and the charge fluctuations of mesoscopic chaotic cavities in terms of a generalized Wigner–Smith matrix. The Wigner–Smith matrix is well known in investigations of time-delay of quantum scattering. It is expressed in terms of the scattering matrix and its derivatives with energy. We consider a similar matrix but instead of an energy derivative, we investigate the derivative with regard to the electric potential. The resulting matrix is then the operator of charge. If this charge operator is combined with a self-consistent treatment of Coulomb interaction, the charge operator determines the capacitance of the system, the non-dissipative ac-linear response, the RC-time with a novel charge relaxation resistance, and in the presence of transport a resistance that governs the displacement currents induced into a nearby conductor. In particular, these capacitances and resistances determine the relaxation rate and dephasing rate of a nearby qubit (a double quantum dot). We discuss the role of screening of mesoscopic chaotic detectors. Coulomb interaction effects in quantum pumping and in photon assisted electron–hole shot noise are treated similarly. For the latter, we present novel results for chaotic cavities with non-ideal leads.

PACS numbers: 73.23.−b, 73.21.La, 05.45.Mt, 21.60.Jz

1. Introduction

Quantum transport in structures so small that the quantum wave nature of particles becomes important presents many theoretical and experimental challenges. The physical realization of such small structures is quite diverse and ranges from electronic transport through (partially) coherent samples [1–5] to scattering of photons in cavities [6, 7] or scattering of particles in compound nuclei [8]. Often the dynamics of particles inside the scattering region is chaotic. In an optical cavity, this is a consequence of the irregular shape of the resonator and, similarly, in electrical samples chaotic scattering results from the boundary or the impurity configuration. This paper, devoted to electron transport, is focused mostly on the particular example of a chaotic cavity, namely a two-dimensional chaotic quantum dot. A typical quantum dot is usually patterned into the two-dimensional electron gas at the interface of semi-conducting

heterostructures. The two-dimensional electron gas results from strong quantization of the electron motion perpendicular to the interface. The shape of the sample is formed with the help of metallic gates on top of the structure. Even if the dot is free of impurities, the shape of the dot is usually quite irregular, so that the dynamics of electrons is classically chaotic. (If in addition there are impurities chaos results independently of the geometric shape of the dot.)

At sufficiently low temperatures, when the length over which the carriers retain phase memory becomes comparable to the dimensions of the structure we enter the regime of *mesoscopic* physics [9, 10]. In this regime, every dot exhibits fluctuating physical properties due to the high sensitivity of quantum interference effects on the exact geometry of the dot. Then properties of small structures must be described by their *statistics* in the form of mesoscopic (sample-to-sample) distribution functions rather than by their averages over ensemble of similarly fabricated samples.

We are interested in dots which are connected to the outside via one or several leads which permit the exchange of carriers with electrical contacts (reservoirs). The connection between the dot and reservoir can be highly transparent or alternatively we can insert tunnel barriers which increasingly insulate the dot from the contacts. If the dot is closed, its equilibrium charge changes in response to the voltage applied to the external gates. Except for special gate voltages, the charge on the dot does not fluctuate. For poorly transmitting contacts (strong tunnel barriers), the charge of the dot is strongly quantized and at low temperatures this quantization can block transport (Coulomb blockade). Such a blockade is important if a typical energy needed to add an electron into a dot, $\sim e^2/C$ (capacitance C defined by geometry), is large compared to the temperature and the escape rate $\gamma_{\rm esc}$ of carriers from the dot, $e^2/C \gg k_{\rm B}T, \hbar\gamma_{\rm esc}$ [9]. However, when the barrier becomes transparent and the contacts are wide open the charge quantization vanishes and weak charge fluctuations appear at all voltages.

The main subject of this paper is the role of Coulomb interactions on transport properties of the dots which are connected with highly transparent contacts to reservoirs. It turns out that in many transport problems the role of Coulomb interactions is closely connected to the Wigner–Smith matrix [11, 12]. This matrix is well known in investigations of the time delay of quantum scattering [13–18]. It is expressed in terms of the scattering matrix and its derivatives with energy. We consider a similar matrix but instead of an energy derivative we investigate the derivative with regard to the electric potential [19, 20]. The resulting matrix is then the operator of charge. If this expression for the charge operator is combined with a description of interaction on the Hartree level (random phase approximation) [21] the charge operator thus found plays an important role in a number of transport problems. The list of these problems includes charge rearrangement in weakly nonlinear transport, the current-response to oscillating potentials, relaxation and dephasing in weakly coupled nearby conductors, the theory of quantum detectors, adiabatic quantum pumping, and frequency-dependent thermal and shot noise.

There are several important questions one might ask: what are the signatures of Coulomb interactions in transport properties of a sufficiently open quantum dot? Which experiment could probe the Coulomb interactions? Can Coulomb effects be distinguished from other effects such as dephasing? Of course for poor contacts, the Coulomb blockade has a very clear signature in transport. However, many experiments are performed with few- and multi-channel open dots, so it is also important to account for Coulomb interactions in such samples.

Our discussion is based on the scattering matrix approach to chaotic systems [22–24]. The formalism is a subject of many extensive reviews [2, 3, 5, 9], and we just outline here why this method is advantageous for our purposes. Our starting point is the energy-dependent scattering matrix $\mathcal{S}(\varepsilon)$ that relates incoming and outgoing electrons at energy ε. This matrix

is obtained from the solution to the Schrödinger equation for *non-interacting* electrons. For low frequencies $\omega \ll \gamma_{\rm esc}$, the scattering matrix varies weakly on the scale $\sim\omega$, so for linear transport one can expand transport coefficients in ω. It is this expansion which makes the Wigner–Smith matrix appear. For quantum dots, the statistical properties of the Wigner–Smith matrix have recently been widely explored [13–18, 25], so that one can use them to find the statistical distribution of measured quantities.

The scattering matrix approach is not the only possible method to solve transport problems. For a discussion of alternative methods and applicability of our approach, we refer to section 9. The self-consistent treatment of the Coulomb interaction is the subject of our paper, and we apply this method even for few-channel quantum dots.

We proceed as follows: in section 2 we first consider non-interacting electrons and introduce the Wigner–Smith matrix as a natural building block for a low-frequency low-temperature transport theory of open cavities. On the example of a single-channel cavity, we demonstrate that taking into account the Coulomb interactions is essential in finite frequency transport. A self-consistent treatment allows us to consider the effect of Coulomb interactions and find the internal potential and its derivative with respect to external perturbations for a dot with arbitrary number of channels. Later we concentrate on applications of our approach to various experimental set-ups. Section 3 considers the role of Coulomb interactions in the renormalization of the effective capacitance and introduces the mesoscopic charge relaxation resistance in terms of the Wigner–Smith matrix. These results are used later in sections 4–8. Section 4 considers the displacement current induced into a nearby gate due to the charge fluctuations associated with shot-noise in a dc-biased two-channel cavity and finds its mesoscopic distribution. In section 5, the relaxation rate and dephasing rate of a charge qubit near a chaotic cavity are discussed. In section 6, we describe how to use these results to describe a quantum detector. Section 7 concerns 'quantum pumps', which pump electrons due a time-periodic variation of the dots shape. The effect of Coulomb interactions on the pumped voltage is considered self-consistently. As another application of the Hartree treatment we consider an ac-biased multi-channel quantum dot in section 8 and find the photon-assisted shot-noise both for completely open dots and partially open dots with equal channel transparencies. In this section, we use results of the appendix for various correlators of the scattering matrices. We discuss other approaches and the applicability of our results in section 9 and conclude in section 10.

2. Generalized Wigner–Smith matrix

In this work, we consider electrical transport problems which can be described with the help of a generalized Wigner–Smith matrix [11, 12]. We illustrate these transport problems for chaotic cavities. In linear response to oscillating potentials the Wigner–Smith matrix describes the leading non-dissipative response and in certain cases also the leading dissipative term. In particular, capacitances [26], charge relaxation resistances [26] and a Schottky resistance in the presence of shot noise [27], can be expressed in terms of interaction constants and the Wigner–Smith matrix.

To be specific, consider the structure in figure 1. A cavity is connected with a single lead to a 'contact'. At the Fermi energy, there are N open quantum channels. As a consequence there exists a scattering matrix $\mathcal{S}$ of dimension $N \times N$ with elements $\mathcal{S}_{mn}$ which relates the current amplitude of the incoming state n to the current amplitudes of the out-going state m. Each carrier incident on the cavity will after some delay be reflected and leave the cavity to be scattered back into the contact. According to Wigner and Smith, the time carriers with energy

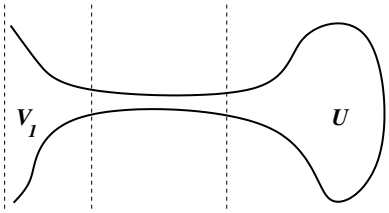

Figure 1. Mesoscopic capacitor connected via a single lead to an electron reservoir. V_1 is the voltage applied to the contact, U is the potential in the cavity.

E spend in the cavity can be found from the matrix,

$$\mathcal{N} = \frac{1}{2\pi \mathrm{i}} \mathcal{S}^\dagger \frac{\mathrm{d}\mathcal{S}}{\mathrm{d}E}. \tag{1}$$

Taking the trace and multiply with Planck's constant gives a sojourn time $\tau_s = h \,\mathrm{tr}\,\mathcal{N}/N$. The time defined in this way depends on how exactly we define the scattering matrix $\mathcal{S}$. We could define $\mathcal{S}$ right at the entrance to the cavity (rightmost broken line in figure 1), somewhere in the long lead, at the entrance to the contact, or even deep inside the contact (leftmost broken line in figure 1). In the original work [12] the $\mathcal{S}$-matrix is clearly defined in an asymptotic way on the surface of a sphere with a radius that is eventually taken to infinity. The time calculated by Smith is a delay, that is a difference of a time in the presence and absence of a scattering centre. This is a sensible procedure if we are not interested exactly where a carrier incurs the delay.

Our aim, however, is to obtain an expression for the *charge*, not the time delay. Moreover, we are interested in the local charge. We have to know, whether this charge is accumulated inside the cavity, in the lead, or inside the contact. Therefore, the Wigner–Smith matrix is not the appropriate object [19, 20]. The *local* question which we are asking can of course also be asked for time. For instance, the widely discussed question, 'how much time does a carrier spend while traversing a tunnel barrier?' is a question about local properties [19, 20] which cannot be answered by an appeal to the Wigner–Smith matrix. It was already noted in the treatment of this problem [28] that instead of using derivatives with regard to energy to find delay, we have to consider derivatives with regard to the electric potential U to find its conjugate, charge. Therefore, consider a small change of the potential inside the cavity only. We can then consider the matrix

$$\mathcal{N} = -\frac{1}{2\pi \mathrm{i}} \mathcal{S}^\dagger \frac{\mathrm{d}\mathcal{S}}{\mathrm{d}(eU)}. \tag{2}$$

Here the $\mathcal{S}$-matrix can be defined asymptotically, i.e. in the contact to the left of figure 1. Nevertheless, the answer given by equation (2) depends now only on the effect which a small change of potential inside the cavity generates. We can now introduce the dwell time [20], which is the total integrated density in the cavity in an energy range $\mathrm{d}E$ divided by the incoming carrier flux $(N/h)\,\mathrm{d}E$

$$\tau_\mathrm{d} = \frac{h}{N} \,\mathrm{tr}\,\mathcal{N} = \mathrm{i}\frac{\hbar}{N} \,\mathrm{tr}\, \mathcal{S}^\dagger \frac{\mathrm{d}\mathcal{S}}{\mathrm{d}(eU)}. \tag{3}$$

We can choose any other potential, in the lead, or in the contact, and ask in a similar way what the dwell time is in the region of interest. We can take the region to be arbitrarily small and instead of a derivative of the $\mathcal{S}$-matrix investigate the functional derivative with regard to the local potential [29–31]. For the purpose of this work, it is, however, sufficient to consider derivatives with regard to single potential U.

Instead of time-delay, or more precisely dwell time, we alternatively use the language of density of states. The density of states inside the cavity is given by

$$\nu = \mathrm{tr}\,\mathcal{N} = -\frac{1}{2\pi\mathrm{i}}\,\mathrm{tr}\left(\mathcal{S}^{\dagger}\frac{\mathrm{d}\mathcal{S}}{\mathrm{d}(eU)}\right) = -\frac{1}{2\pi\mathrm{i}}\frac{\mathrm{d}}{\mathrm{d}(eU)}\ln(\det\mathcal{S}), \tag{4}$$

where U is the potential in the cavity. If ν is multiplied by an energy interval $\mathrm{d}E$ and the charge e, then $\Delta Q = e\nu\,\mathrm{d}E$ is the charge in the cavity due to the incident scattering states in the interval $\mathrm{d}E$. Importantly this is the charge of non-interacting carriers. A conductor, when charged, will respond with an induced electrical potential U to bring the charge in a given region to the value permitted by the Coulomb interaction.

Suppose that we consider the linear response of the current in the contact $\mathrm{d}I(t) = \mathrm{d}I(\omega)\exp(-\mathrm{i}\omega t)$ to an oscillating potential applied to the contact of the sample, $\mathrm{d}V(t) = \mathrm{d}V(\omega)\exp(-\mathrm{i}\omega t)$. In the zero-temperature limit, the response is to leading orders in frequency,

$$G(\omega) = \mathrm{d}I(\omega)/\mathrm{d}V(\omega) = -\mathrm{i}\omega e^2\,\mathrm{tr}\,\mathcal{N} + \omega^2(e^2/2h)\,\mathrm{tr}\,\mathcal{N}^2 + O(\omega^3). \tag{5}$$

The first term is a non-dissipative response determined by the density of states ν of the cavity. $e^2\nu$ has the the dimension of capacitance and is called the quantum capacitance [26, 32–34], $C_q = e^2\nu$. The second term is real and thus represents the leading dissipative part of the response.

Equation (5) is not, however, a physically acceptable result already for the geometry shown in figure 1. It is necessary to consider the fact that electrons are interacting particles. To see the problem, suppose that the cavity and/or the lead are charged above what the ionic background of the conductor permits. As a consequence there will be long-range electrical field lines emanating from the cavity and the lead. However, if the contact, the lead, and the cavity are the only metallic bodies, the electrical field lines emerging from the cavity or the lead will eventually end on the metallic contact. There exists, therefore, a Gauss volume taken large enough such that the electrical flux through its surface vanishes. The charge inside this Gauss volume is a constant of motion. Instead of equation (5) we should find $G(\omega) = 0$. We can see the profound effect of the long-range Coulomb interaction in another way. The particle current density $I^{\mathrm{p}}(\mathbf{r}, t)$ is not necessarily a conserved quantity. But if we add the Maxwell displacement current $I^{\mathrm{d}}(\mathbf{r}, t) = \epsilon_L\,\mathrm{d}E(\mathbf{r}, t)/\mathrm{d}t$ with $E(\mathbf{r}, t)$ the electric field and consider the total current $I^{\mathrm{tot}}(\mathbf{r}, t) = I^{\mathrm{p}}(\mathbf{r}, t) + I^{\mathrm{d}}(\mathbf{r}, t)$ we have a quantity of vanishing divergence, $\mathrm{div}\, I^{\mathrm{tot}}(\mathbf{r}, t) = 0$. The total current has no sources or sinks. It is important to emphasize that it is the total current that is measured in experiment. Thus equation (5), valid for non-interacting carriers, is on physical grounds unacceptable.

We now consider a more general arrangement and explain how the self-consistent Coulomb potential is determined. We consider transport through a dot with several contacts at which voltages $V_\alpha(t) = V_\alpha\cos(\omega t + \phi_\alpha)$ at some frequency ω are applied. In the end, our results are also applicable for dc transport, if the limit $\omega \to 0$ is taken. In fact, in a dc-biased system, within linear transport, the potential $U(t) = \mathrm{const}$ and is not important, since at zero frequency, $\omega = 0$, the current is gauge invariant and knowledge of the internal potential is not necessary. However, its derivative with respect to an external perturbation in the αth lead, $\mathrm{d}U/\mathrm{d}V_\alpha$, can be used, e.g. in the analysis of the magnetic field asymmetry of the current in the nonlinear transport through a dot [35]. As described above, the charge inflow into the dot shifts the internal potential $U(t)$ due to capacitive coupling to the gate C, kept at a potential $V_0(t) = V_0\cos(\omega t + \phi_0)$.

The current $I_\alpha(\Omega)$ at finite frequency Ω in the αth lead attached to the dot is the sum of two contributions: particle current $I^{\mathrm{p}}_\alpha(\Omega)$ and displacement current $I^{\mathrm{d}}_\alpha(\Omega)$. The former is due to variations of electro-chemical potentials in various leads and is expressed via conductances

$G_{\alpha\beta}(\Omega)$ [26] of non-interacting electrons

$$G_{\alpha\beta}(\Omega) = \frac{e^2}{h}\int \mathrm{d}\varepsilon\, \mathrm{tr}(\delta_{\alpha\beta}\mathbf{1}_\alpha - \mathbf{1}_\alpha \mathcal{S}^\dagger(\varepsilon)\mathbf{1}_\beta \mathcal{S}(\varepsilon+\hbar\Omega))\frac{f(\varepsilon)-f(\varepsilon+\hbar\Omega)}{\hbar\Omega}. \tag{6}$$

Here we introduce the matrices $\mathbf{1}_\alpha$ which have unit elements along the diagonal of the channels of contact α and zero otherwise. The displacement current, the result of screening, corresponds to variations of charge inside the dot and is expressed through the potential $U(\Omega)$ and yet unknown susceptibility $\chi_\alpha(\Omega)$. Thus the current at probe α is

$$I_\alpha(\Omega) = I_\alpha^{\mathrm{p}}(\Omega) + I_\alpha^{\mathrm{d}}(\Omega) = \sum_\beta G_{\alpha\beta}(\Omega)V_\beta(\Omega) + \chi_\alpha(\Omega)U(\Omega). \tag{7}$$

We require gauge-invariance, that implies that the global shift of all potentials $V_i(\Omega) \to V_i(\Omega) - f(\Omega)$, $U(\Omega) \to U(\Omega) - f(\Omega)$ by an arbitrary $f(\Omega)$ does not change the *total* current [26]. This determines the susceptibility, $\chi_\alpha(\Omega) = -\sum_\beta G_{\alpha\beta}(\Omega)$. As a consequence, the current depends on difference of potentials only, as expected:

$$I_\alpha(\Omega) = \sum_\beta G_{\alpha\beta}(\Omega)(V_\beta(\Omega) - U(\Omega)). \tag{8}$$

On the other hand, from charge conservation $\sum_\alpha I_\alpha(t) = C(\mathrm{d}/\mathrm{d}t)[V_0(t) - U(t)]$, we find that $U_\Omega \neq 0$ only at $\Omega = \pm\omega$. In response to potentials with Fourier components $V_{\alpha,\omega} = V_\alpha \exp(\mathrm{i}\phi_\alpha)$ the frequency-dependent potential U_ω is

$$U_\omega = \frac{\sum_{\alpha\beta} G_{\alpha\beta}(\omega)V_{\beta,\omega} + \mathrm{i}\omega C V_{0,\omega}}{\sum_{\alpha\beta} G_{\alpha\beta}(\omega) + \mathrm{i}\omega C}. \tag{9}$$

At low frequencies, which is often important, the scattering matrices $\mathcal{S}$ are weakly dependent on energy, and the first terms in an expansion of the scattering matrix in energy are sufficient to evaluate the potential U_ω and the partial derivative of U_ω with respect to the potential $V_{\alpha,\omega}$. With the Wigner–Smith matrix $\mathcal{N}$ introduced in equation (1) and the matrix of voltages $\hat{V}_\omega = \sum_\alpha \mathbf{1}_\alpha V_{\alpha,\omega}$ the sample-specific expressions read

$$U_\omega - V_{0,\omega} = \frac{\mathrm{tr}\,\mathcal{N}(\hat{V}_\omega - \mathbf{1}V_{0,\omega})}{C/e^2 + \mathrm{tr}\,\mathcal{N}}, \qquad \frac{\partial U_\omega}{\partial V_{\alpha,\omega}} = \frac{\mathrm{tr}\,\mathcal{N}\mathbf{1}_\alpha}{C/e^2 + \mathrm{tr}\,\mathcal{N}}. \tag{10}$$

Both quantities naturally vanish in the non-interacting limit $C \to \infty$ and reach a finite value in the opposite, strongly-interacting limit, $C \to 0$. In the following, we use this approach to calculate several transport properties.

3. Capacitance and charge relaxation resistance

Figure 2 shows a single-lead cavity which is separated by an insulating material from a back gate at voltage $V_0(t)$. Now we have the possibility of driving an ac-current through the system. In addition to the current response to $V_1(t)$, we can investigate the response to $V_0(t)$. A consistent treatment of the long-range Coulomb interaction demands that these two responses are different only in sign. In fact the response must depend only on the voltage difference $V(t) = V_1(t) - V_0(t)$; see equation (10). Here we describe the Coulomb interaction in simple terms using a geometrical capacitance C which links the potential difference between cavity and gate and the charge on the cavity and the gate. As a consequence, the conductance of the cavity capacitively coupled to a gate is now given by

$$G(\omega) = -\mathrm{i}\omega C_\mu + \omega^2 C_\mu^2 R_q + O(\omega^3). \tag{11}$$

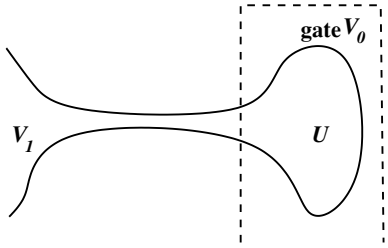

Figure 2. Mesoscopic capacitor connected via a single lead to an electron reservoir and capacitively coupled to a gate. V_1 and V_0 are the potentials applied to the contacts, U is the electric potential of the cavity.

Here the first term is the electro-chemical capacitance [26] which is the series capacitance of the geometrical capacitance C and the 'quantum capacitance' νe^2,

$$C_\mu^{-1} = C^{-1} + (\nu e^2)^{-1}. \tag{12}$$

Thus the capacitance is not a purely geometrical quantity, but depends via the density of states ν on the properties of the specific electrical conductor. Note that C_μ^{-1} is a fluctuating quantity, with mesoscopic average equal to $\langle 1/C_\mu \rangle = 1/C + \Delta/e^2$. Here Δ is the mean level spacing in the dot. Equation (12) has important implications: for instance, if the cavity is deformed into a ring with an Aharonov–Bohm flux through the hole of the ring, the capacitance exhibits quantum oscillations which are periodic in the flux [36, 37]. Such oscillations have been observed in arrays of rings by Deblok *et al* [38] and in a strikingly clear manner on a single mesoscopic capacitor by Gabelli *et al* [39].

The second, dissipative term, is governed by a resistance R_q which we call a charge relaxation resistance [26]:

$$R_q = \frac{h}{2e^2} \frac{\mathrm{tr}\,\mathcal{N}^2}{\mathrm{tr}^2\,\mathcal{N}}. \tag{13}$$

Equations (12) and (13) are given in the low temperature limit $k_B T \ll \hbar\omega$. To understand the meaning of these quantities better, it is instructive to consider a basis in which the scattering matrix is diagonal. All eigenvalues of the scattering matrix are of the form $\exp(i\zeta_n)$ where ζ_n is the phase which a carrier accumulates from multiple scattering inside the cavity. Thus the density of states (4) can also be expressed as

$$\nu = -(1/2\pi) \sum_n (\mathrm{d}\zeta_n/\mathrm{d}(eU)). \tag{14}$$

Similarly we can express the charge relaxation resistance in terms of the potential derivatives of phases. In the low temperature limit, R_q is determined by the sum of the squares of the dwell times divided by the square of the sum of the dwell times,

$$R_q = \frac{h}{2e^2} \frac{\sum_n (\mathrm{d}\zeta_n/\mathrm{d}(eU))^2}{\left(\sum_n \mathrm{d}\zeta_n/\mathrm{d}(eU)\right)^2}. \tag{15}$$

We now briefly discuss the charge relaxation resistance. First we note that the resistance unit is not the resistance quantum h/e^2 but $h/2e^2$. The factor 2 arises since the cavity is coupled to one reservoir only. Thus only half the energy is dissipated as compared to dc-transport through a two terminal conductor. We emphasize that the factor 2 is not connected to spin: $h/2e^2$ results from a single spin polarized channel. In the single channel limit, equation (15) is *universal* and given just by $h/2e^2$. This is astonishing since if we imagine that a barrier

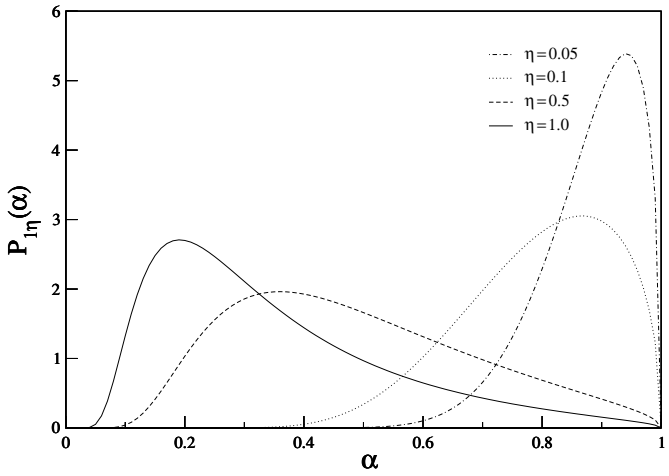

Figure 3. Mesoscopic capacitance distribution $P_{1\eta}(\alpha)$ of a cavity connected via a single perfect lead to a reservoir. The capacitance is in units of the geometric capacitance, $\alpha = C_\mu/C$. The ratio $\eta = \Delta(C/e^2)$ is the level spacing in units of the Coulomb energy (after [14]).

is inserted into the lead connecting the cavity to the reservoir one would expect a charge relaxation resistance that increases as the transparency of the barrier is lowered. Indeed, if there is a barrier with transmission probability $\mathcal{T}$ per channel in the lead connecting the cavity and the reservoir, then in the large channel limit, for $\mathcal{T}N \gg 1$, R_q is

$$R_q = (h/e^2)(1/\mathcal{T}N). \tag{16}$$

In the large-channel limit, equation (16) is inversely proportional to the total transmission $N\mathcal{T}$. Thus in the large channel limit equation (15) behaves as expected. For a one-channel connection to a reservoir the recent experiment by Gabelli *et al* [39] indeed finds a resistance of 12 kΩ for a mesoscopic capacitor formed with the help of a quantum point contact in high magnetic fields in the quantum Hall regime. A brief overview of charge relaxation resistances in mesoscopic systems is presented in [40].

For a single channel connected to a cavity, the charge relaxation resistance is universal and given by $h/2e^2$. Thus it is only the capacitance C_μ which needs to be investigated further. Gopar, Mello and one of the authors [14] and independently Fyodorov and Sommers [13] calculated the distribution of dwell times $w_\beta(\tau_d)$ for a cavity coupled to a lead with a perfect one-channel quantum contact in the cases of time reversal, broken time-reversal and broken spin-inversion symmetry (denoted by Dyson symmetry indices $\beta = 1, 2, 4$ respectively [41]). This permits us to find the distribution function of the capacitance (12) of such a cavity. Figure 3 shows the distribution $P_{1\eta}(\alpha)$ in the presence of time-reversal symmetry, $\beta = 1$, of $\alpha = C_\mu/C = \tau_d/(\tau_d + \eta)$ where $\eta = C\Delta/e^2$ is the ratio of the level spacing and Coulomb energy. The distributions for larger η are wider, because with $\eta \to \infty$ the mesoscopic fluctuations of ν have a stronger effect on C_μ. Typically the Coulomb energy is much larger than the level spacing, the parameter η is small and the capacitances are close to the geometrical value (see figure 3).

Next let us consider a cavity that is connected via $N = 2$ open quantum channels to the outside. The two open channels can be provided by the same contact (a single lead as in figure 2) or from different contacts as shown in figure 4. There are now two dwell times which in general differ from one another. Their joint distribution (for arbitrary N) is derived

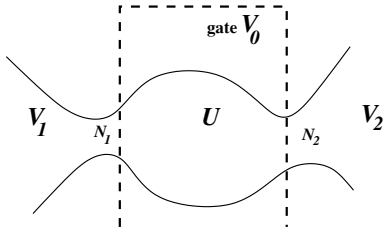

Figure 4. Chaotic dot connected via two quantum point contacts with N_1 and N_2 open quantum channels. The dot is capacitively coupled to a gate at voltage V_0.

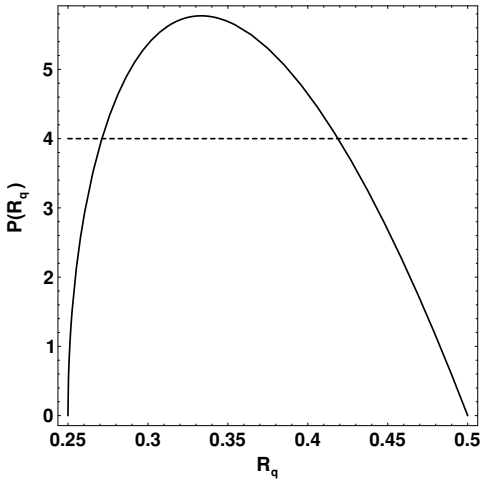

Figure 5. Charge relaxation resistance R_q, measured in units of h/e^2, for $\beta = 1$ (dashed curve) and $\beta = 2$ (solid) (after [27]).

in [18]. As a consequence, we now have a nontrivial distribution also of the charge relaxation resistance [27] shown in figure 5. For the case of time-reversal symmetry, $\beta = 1$, reference [27] finds that R_q is uniformly distributed between $R_q = h/4e^2$ and $R_q = h/2e^2$, whereas for the broken time-reversal symmetry, $\beta = 2$, the distribution exhibits a peak and reaches zero at the limiting values [27]. The limiting values are reached if both channels have dwell times close to each other ($R_q = h/4e^2$) and if one of the dwell times becomes very much longer than the other one ($R_q = h/2e^2$). The probability of such processes for $\beta = 1$ is higher then at $\beta = 2$, so that the distributions are stronger at $R_q = h/2e^2, h/4e^2$.

4. Charge noise in the presence of shot noise

We have derived the capacitance C_μ and the charge relaxation resistance R_q from linear response. The dissipative part of the response proportional to R_q is related to the charge and current fluctuations of the system via the fluctuation dissipation-theorem. Returning to the single-lead configuration in figure 2, we can calculate the current fluctuations at contact $\alpha = 1$ or at the gate $\alpha = 0$ or their correlations, $S_{\alpha\beta}(t) = 1/2 \int dt' \langle\langle I_\alpha(t+t')I_\beta(t) + I_\beta(t)I_\alpha(t+t')\rangle\rangle$. Due to current conservation, we have $S(t) \equiv S_{11}(t) = S_{00}(t) = -S_{10}(t) = -S_{01}(t)$. For the Fourier transform of this noise spectrum, we have $S_{II}^{\rm eq}(\omega) = 2k_{\rm B}T\omega^2 C_\mu^2 R_q$, where we have taken the classical limit $\hbar\omega \ll k_{\rm B}T$. Since the current is the time derivative of the charge

accumulated on the cavity, we immediately also find the spectrum of the charge fluctuations Q on the cavity, $S^{\rm eq}_{QQ}(\omega) = 2k_{\rm B}TC_\mu^2 R_q$.

Next consider the case of a cavity with two contacts which permit exchange of carriers with reservoirs, as shown in figure 4. There N_1 quantum channels in the QPC connect the cavity to the left contact at voltage V_1 and N_2 quantum channels connect the cavity to the right at contact 2 with voltage V_2. If these two voltages differ, a transport state is established. At zero temperature, we have a current $I = GV$ with $V = V_1 - V_2$ determined by the Landauer formula, $G = (e^2/h)\mathcal{T}$ where $\mathcal{T} = {\rm tr}\,\mathcal{S}^\dagger \mathbf{1}_2 \mathcal{S}\mathbf{1}_1$. For a chaotic cavity, the ensemble averaged total transmission probability is $\mathcal{T} = N_1N_2/(N_1 + N_2)$. For simplicity, we consider a voltage $eV \gg k_{\rm B}T$ so large that the thermal noise in this conductor can be neglected. However, the granularity of charge and the fact that to every incident channel there are different final channels leads to shot noise [4] with a zero-frequency noise spectrum given by $S_{II}^{\rm shot} = 2e(e^2/h)|V|\,{\rm tr}(\mathbf{1}_1\mathcal{S}^\dagger\mathbf{1}_1\mathcal{S}\mathbf{1}_1\mathcal{S}^\dagger\mathbf{1}_2\mathcal{S})$. In terms of the transmission eigenvalues, the shot noise is $S_{II}^{\rm shot} = 2e(e^2/h)|V|\sum_n T_n(1-T_n)$. For a chaotic cavity with large perfect quantum point contacts $N_1, N_2 \gg 1$, the ensemble averaged shot noise [4, 24, 42] is $S_{II}^{\rm shot} = 2e(e^2/h)|V|N_1^2N_2^2/(N_1+N_2)^3$. For single channel leads $N_1 = N_2 = 1$, the case of interest here, shot noise is characterized by a distribution which is given in [27]. The stochastic transfer of carriers through the cavity leads to fluctuations of the charge in the cavity as a function of time. Such charge fluctuations can build up only if screening in the conductor is not perfect. Therefore, consider now again a nearby gate which is capacitively coupled to the conductor with a geometric capacitance C. The fluctuating charge in the cavity induces charge fluctuations in the nearby gate such that the charge on the conductor and the gate is conserved. In the transport situation considered here, the different voltages in the leads break the symmetry between contacts. An important role is now played by certain selected elements of the full Wigner–Smith matrix. The elements which retain information on the contacts from which carriers are incident are

$$\mathcal{N}_{\beta\gamma}(E) = -\frac{1}{2\pi{\rm i}}\left(\mathcal{S}^\dagger(E)\frac{{\rm d}\mathcal{S}(E)}{{\rm d}(eU)}\right)_{\beta\gamma}. \tag{17}$$

Introducing the second quantization operators $\hat{a}_\beta(E)$ which annihilate an electron in the incoming channel in lead β, we write the charge operator [27] in the absence of interaction as

$$e\hat{\mathcal{N}} = e\mathcal{N}_{\beta\gamma}(E)\hat{a}^\dagger_\beta(E)\hat{a}_\gamma(E). \tag{18}$$

In reality the Coulomb interaction leads to potential fluctuations inside the cavity and these fluctuations contribute in turn to the charge. Since charge and potential are linearly related, we are led to describe the fluctuating potential also with an operator $\hat{U}$ that contributes to the net charge in proportion to the density of states ν in the cavity. We have $\hat{Q}_{\beta\gamma} = e\hat{\mathcal{N}}_{\beta\gamma} - e^2\nu\hat{U}_{\beta\gamma}$. On the other hand, the Coulomb interaction dictates that $\hat{Q}_{\beta\gamma} = C\hat{U}_{\beta\gamma}$. Taken together, we have therefore,

$$\hat{Q}_{\beta\gamma} = C\hat{U}_{\beta\gamma} = e\hat{\mathcal{N}}_{\beta\gamma} - e^2\nu\hat{U}_{\beta\gamma}. \tag{19}$$

Solving for $\hat{U}_{\beta\gamma}$ determines the charge fluctuations in the presence of screening,

$$\hat{Q}_{\beta\gamma} = \frac{Ce\hat{\mathcal{N}}_{\beta\gamma}}{(C+\nu e^2)} = e\frac{C_\mu}{\nu e^2}\hat{\mathcal{N}}_{\beta\gamma}. \tag{20}$$

Here C_μ is the electro-chemical capacitance, equation (12). Evaluation of the quantum statistical expectation value leads to a low-frequency charge-fluctuation spectrum $S_{QQ}(0) = 2e|V|C_\mu^2 R_v$ determined by the resistance [27]

$$R_v = \frac{h}{e^2}\frac{{\rm tr}\,\mathcal{N}\mathbf{1}_1\mathcal{N}\mathbf{1}_2}{{\rm tr}^2\,\mathcal{N}}. \tag{21}$$

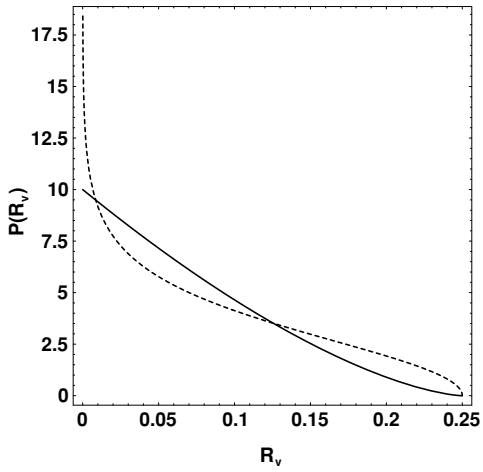

Figure 6. Distribution of the resistance R_v which determines the low-frequency charge fluctuation spectral density of a chaotic cavity connected to reservoirs with two single channel leads. Dashed line is for the orthogonal ensemble, $\beta = 1$, solid line is for the unitary ensemble, $\beta = 2$ (after [27]).

For a chaotic cavity connected only to two single channel leads the distribution of the resistance R_v is shown in figure 6. In many cases, the mesoscopic distribution $P(C_\mu)$ of the electrochemical capacitance C_μ is much narrower than that of R_v (cf figure 3 for small η and figure 6), and the fluctuations of noise S_{QQ} are mostly due to fluctuations of R_v.

It is interesting to calculate not only the spectrum of the noise induced into the gate but also the spectrum at the contacts which connect the cavity to reservoirs. Extending the discussion of [27] Hekking and Pekola [43] find the finite frequency noise spectra in the quantum limit. A quasi-classical discussion of the frequency-dependent third cumulant of chaotic cavities is given by Nagaev, Pilgram, and one of the authors [44]. It turns out that in higher cumulants both the RC-time and the dwell time are relevant [44]. For a related discussion of dynamical thermal effects, we refer the reader to Reulet and Prober [45].

5. Relaxation and dephasing rate of a charge qubit

To illustrate the physical significance of the charge relaxation resistance (13) and the resistance R_v (21), we now consider a chaotic cavity coupled capacitively to a double quantum dot as shown in figure 7. The double dot represents a charge qubit: a single charge tunnels between the upper and lower dots. The chaotic cavity plays the role of a detector. With this set-up, we can investigate the question [46]: if we use a generic mesoscopic conductor (here a chaotic cavity) how good a detector would this represent? The properties and suitability of special systems, such as quantum point contacts or single electron transistors, as detectors have been widely discussed [30, 46–55] and continue to be the subject of research [56–60]. Interestingly a chaotic cavity connected to one channel leads is with a probability of almost one-half close to an ideal detector and if it is not ideal changing the shape of the cavity just a bit leads with probability of one-half to an almost ideal detector [46].

The two-level system is represented by the Hamiltonian $\hat{H}_{DD} = \frac{\epsilon}{2}\hat{\sigma}_z + \frac{\Delta}{2}\hat{\sigma}_x$, where $\hat{\sigma}_i$ denote Pauli matrices. The energy difference between upper and lower dots is ϵ and Δ accounts for tunnelling between the dots. The full level splitting is thus $\Omega = \sqrt{\epsilon^2 + \Delta^2}$. The chaotic

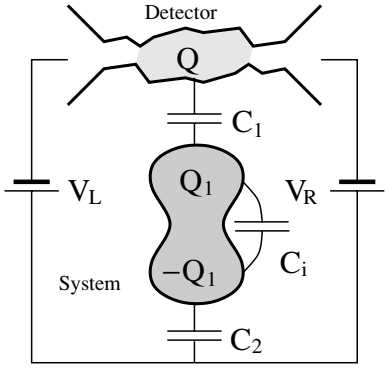

Figure 7. Chaotic cavity capacitively coupled to a double quantum dot (after [46]).

cavity and the two-level system are coupled through the long-range Coulomb interaction taken into account with a set of capacitances C_1, C_2, C_i that link the charge Q_1 and $-Q_1$ on the double dot to the charge on the cavity. The series capacitance is $C^{-1} = C_1^{-1} + C_2^{-1} + C_i^{-1}$.

If the two-level system is in a superposition state, it experiences relaxation with a rate $\Gamma_{\rm rel}$ towards the ground state due to charge fluctuations in the cavity. In addition, a coherent state of the two-level system is dephased with a rate $\Gamma_{\rm dec}$.

At equilibrium the relaxation rate and decoherence rate generated by the cavity are determined by the charge relaxation resistance [46]

$$\Gamma_{\rm rel} = 2\pi \frac{\Delta^2}{\Omega^2} \left(\frac{C_\mu}{C_i}\right)^2 R_q \frac{\Omega}{2} \coth \frac{\Omega}{2k_{\rm B}T}, \tag{22}$$

$$\Gamma_{\rm dec} = \frac{\Gamma_{\rm rel}}{2} + 2\pi \frac{\epsilon^2}{\Omega^2} \left(\frac{C_\mu}{C_i}\right)^2 R_q k_{\rm B} T. \tag{23}$$

A charge relaxation resistance exists even if the conductor permits no transmission of carriers. Often the interaction of a qubit and a detector is modelled by describing the effect of the qubit solely in terms of a modulation of the transmission amplitude of the conductor. Such a description predicts that a conductor with zero transmission probability causes no relaxation and no dephasing. But a conductor with transmission probability zero is just a capacitor, and, as we have seen, a mesoscopic capacitor has a non-vanishing charge relaxation resistance.

In the zero-temperature limit, the two-level system relaxes due to the zero-point fluctuations of the conductor. A qubit in an excited state is a detector of vacuum fluctuations. If a voltage is applied to the conductor, the decoherence rate contains in addition a term which arises due to the charge fluctuations in the presence of shot noise of the detector. This additional term is proportional to the applied voltage and is governed by R_υ,

$$\Gamma_{\rm dec} = \frac{\Gamma_{\rm rel}}{2} + 2\pi \frac{\epsilon^2}{\Omega^2} \left(\frac{C_\mu}{C_i}\right)^2 R_\upsilon e|V|. \tag{24}$$

Thus the density of states of the cavity ν, its electro-chemical capacitance C_μ, and the two resistances R_q and R_υ are the properties of the mesoscopic conductor which determine the relaxation and decoherence rate of the two-level system.

6. Chaotic cavity as a quantum detector

The cavity in figure 7 can be viewed as a detector of the state of the two-level system. The current through the cavity depends on whether the charge Q_1 is close to the cavity or in the dot further away from the cavity. The difference of the currents $\Delta I = I_1 - I_2$ is evaluated using the Landauer formula

$$\Delta I = \Delta G|V| = \frac{e^2}{2\pi}|V| \sum \frac{\mathrm{d}T_n}{\mathrm{d}(eU)}(e\Delta U) \tag{25}$$

where ΔG is the change of conductance between the two states of the double dot and $\Delta U = eC_\mu/((\nu e^2)(C_i - C_\mu))$ is the potential change on the mesoscopic conductor [46]. To measure the current, the shot noise of the cavity must be overcome. The zero-frequency shot noise is $S_{II} = e|V|(e^2/2\pi)\sum T_n(1 - T_n)$. Therefore, a measurement time [51, 54] $\tau_m = 4S_{II}/(\Delta I)^2$ is needed for a signal-to-noise ratio of 1. Using weak coupling $C_1, C_2 \ll C_i$ one gets for the inverse measurement time [46]

$$\tau_m^{-1} = \Gamma_m = 2\pi \left(\frac{C_\mu}{C_i}\right)^2 R_m e|V| \tag{26}$$

with the resistance

$$R_m = \frac{h}{4e^2} \frac{\left(\sum_n \mathrm{d}T_n/\mathrm{d}(eU)\right)^2}{\left(\sum_n \mathrm{d}\phi_n/\mathrm{d}(eU)\right)^2 \sum_n T_n(1 - T_n)}. \tag{27}$$

Fundamentally the measurement is always slower than the decoherence, the decay of the off-diagonal elements of the reduced density matrix of the two-level dot. This implies the inequality $\Gamma_m \leqslant \Gamma_{\mathrm{dec}}$ or $R_m \leqslant R_v$. This can be shown by deriving a Schwarz inequality for a combination of scattering matrices and the element $\mathcal{N}_{21}$ of the Wigner–Smith matrix (see [46]) or more generally within linear response detector theory [55].

An efficient detector provides a maximum of information for a minimum of back-action (i.e. decoherence) on the measured system [55]. The efficiency of the detector is determined by the ratio $\eta = \Gamma_m/\Gamma_{\mathrm{dec}} = R_m/R_v \leqslant 1$. The most efficient measurement requires that the tunnelling between the two double dots is negligible, $\Delta \simeq 0$, and the temperature must be much smaller than the applied voltage $k_{\mathrm{B}}T \ll e|V|$. But more importantly with the general formulation given above, we can now discuss the conditions on the scattering matrix for the detector to be ideal. Reference [46] finds that the scattering matrix needs to be of block-diagonal form: channel mixing detectors are not ideal. Consequently the scattering matrix of an ideal detector can be divided into 2×2 blocks of the form

$$s^{(n)} = \begin{pmatrix} -\mathrm{i}\sqrt{1 - T_n}\,\mathrm{e}^{\mathrm{i}(\phi_n + \phi_{A,n})} & \sqrt{T_n}\,\mathrm{e}^{\mathrm{i}(\phi_n - \phi_{B,n})} \\ \sqrt{T_n}\,\mathrm{e}^{\mathrm{i}(\phi_n + \phi_{B,n})} & -\mathrm{i}\sqrt{1 - T_n}\,\mathrm{e}^{\mathrm{i}(\phi_n - \phi_{A,n})} \end{pmatrix}. \tag{28}$$

Each block is defined by its transmission probability T_n and three scattering phases $\phi_n, \phi_{A,n}, \phi_{B,n}$. Using the definition of R_v (equation (21)), we arrive at [27]

$$R_v = \frac{h}{e^2} \frac{\sum_n ((\mathrm{d}T_n/\mathrm{d}U)^2/(4T_n(1 - T_n)) + T_n(1 - T_n)(\mathrm{d}(\phi_{A,n} - \phi_{B,n})/\mathrm{d}U)^2)}{\left(\sum_n \mathrm{d}\phi_n/\mathrm{d}U\right)^2}. \tag{29}$$

Equation (29) reduces to earlier results [47, 51, 52] in the infinite capacitance limit where $C_\mu^2 R_v$ in equation (4) can be replaced by $R_v(\nu e^2)^2$. In equation (29), the derivatives $\mathrm{d}T_n/\mathrm{d}(eU)$ determine the sensitivity of the cavity to a potential variation ΔU. A high sensitivity implies a fast detector (a short measurement time). However, a high sensitivity also implies a fast decoherence rate proportional to R_v. From this, we see that decoherence and measurement speed are closely related quantities.

Demanding that R_m and R_v are equal, requires $\mathrm{d}\phi_{A,n}/\mathrm{d}U - \mathrm{d}\phi_{B,n}/\mathrm{d}U = 0$. As pointed out by Clerk, Girvin and Stone [55], this condition is not connected to any physical symmetry of the system, but can be understood as a condition that the detector should not transfer information into the phases of the scattered electrons since these are not measured. However, we can require that each individual phase-dependent term vanishes separately. $\mathrm{d}\phi_{B,n}/\mathrm{d}(eU) = 0$ in equation (29) can be achieved by requiring that the scattering Hamiltonian must obey time-reversal symmetry. The phases $\mathrm{d}\phi_{A,n}/\mathrm{d}(eU) = 0$ vanish for detectors that obey a spatial inversion symmetry $V(x, y, z) = V(x, y, -z)$. (Here we assume that conduction is along z and x, y are transverse coordinates.) Interestingly, reference [46] finds that in the multichannel case $N > 1$ another condition is needed! The equality $R_m = R_v$ gives us a condition which is of statistical origin. The total conductance of the detector is a sum of one-channel conductances that have independent uncertainties. The statistical uncertainty of this sum is minimized if [46],

$$\frac{\mathrm{d}T_n}{T_n(1-T_n)} = C(U)\,\mathrm{d}(eU), \tag{30}$$

with a function $C(U) > 0$ that does not depend on the index n. In the WKB limit, we have $\mathrm{d}/\mathrm{d}E = -\partial/\partial(eU)$ and equation (30) can be interpreted as differential equations for the transmission probabilities $T_n(E)$. The solutions are all of the form $T_n = (1+\mathrm{e}^{-(F(E)-F(E_n))})^{-1}$ with $\mathrm{d}F/\mathrm{d}E = C$. (The function F is therefore monotonously increasing.) The only difference allowed between the different probabilities T_n is the offset energy E_n. Transmission probabilities of type (30) occur automatically if the scattering problem is separable due to a potential of shape

$$V(x, y, z) = Z(z) + W(x, y). \tag{31}$$

This occurs in particular for the case $F = 2\pi E/\omega_z$ with a symmetric harmonic scattering potential $Z(z) = V_0 - m\omega_z^2 z^2/2$ which is the saddle-point potential of an ideal quantum point contact.

To illustrate the role of the condition equation (31), we now consider chaotic cavities as detectors. The condition equation (31) states that a geometry with a separable potential $V(x, y, z) = Z(z) + Y(x, y)$ is favourable to obtain an efficient detector in the case of more than one open channel. It is clear that a chaotic cavity violates this condition. The efficiency $\eta = \Gamma_m/\Gamma_v = R_m/R_v$ of a chaotic detector with two open channels in each contact is expected to be much smaller than a chaotic cavity connected to single channel contacts for which equation (31) plays no role.

Using the distribution of the elements of the Wigner–Smith matrix (the Laguerre ensemble [17]), we find the probability distribution of the measurement efficiency $\eta = R_m/R_v$ in the orthogonal (time-reversal symmetry) and unitary ensemble (broken time-reversal symmetry) shown in figure 8. The distribution for $N_1 = N_2 = 1$ in the unitary ensemble can also be calculated analytically, $P(\eta) = 1/\sqrt{\eta(1-\eta)}$. The distributions for the other cases were obtained by numerical integration. Interestingly figure 8 shows that despite the absence of inversion symmetry a chaotic dot with open single-channel contacts is with high probability an efficient detector! It is clearly visible that chaos reduces strongly the efficiency of the measurement device as soon as more than one channel contributes to the electric transport. Compared to the time-reversal symmetric case (solid curve in the upper panel) the reduction due to a broken time-reversal symmetry (solid curve in the bottom panel) is much less pronounced.

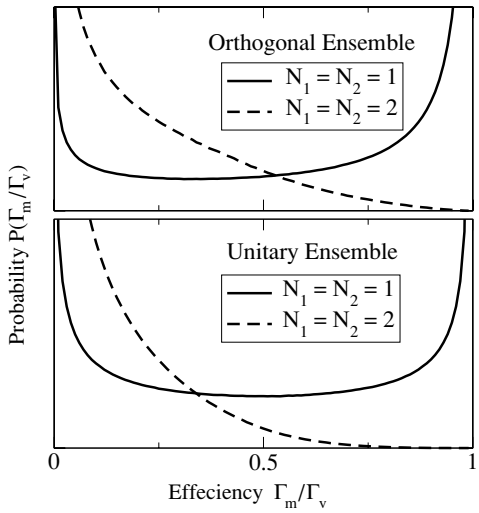

Figure 8. Efficiency distribution of an ensemble of chaotic quantum cavity detectors: orthogonal ensemble (top panel), unitary ensemble (lower panel) for single channel ($N_1 = N_2 = 1$) and double channel ($N_1 = N_2 = 2$) point contacts (after [46]).

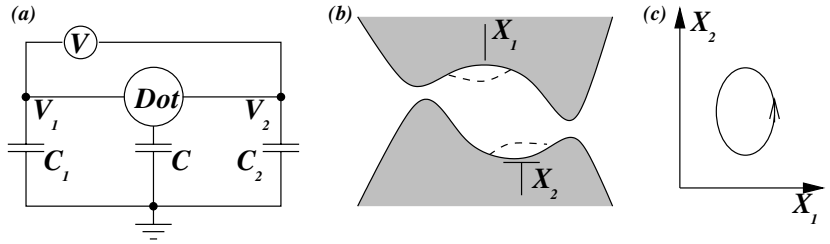

Figure 9. (a) Schematics of the voltage measurement set-up: quantum dot and reservoirs with potentials $V_{1(2)}$ are capacitively coupled to the ground via C and $C_{1(2)}$; (b) weak time-dependent potentials $X_{1,2}(t)$ generate pumped dc current (voltage); (c) the pumped voltage $\bar{V}$ is proportional to the area of the contour in parameter space of the voltages $X_{1,2}(t) = X_{1,2}\cos(\omega t + \phi_{1,2})$ (shown for $\phi_1 - \phi_2 = \pi/2$).

7. Quantum pumping

Quantum pumping exploits the sensitivity of quantum interference to variations of parameters of the scattering matrix. The variation of two parameters $X_{1,2}(t) = X_{1,2}\cos(\omega t + \phi_{1,2})$ oscillating with the same frequency but out of phase generates a dc-current [61–68], if the oscillating scatterer is in a zero-impedance external circuit, or a dc-voltage [69] (if the pump operates in an external circuit with finite impedance). Oscillating parameters $X_{1,2}$ are due to, e.g. voltages applied to the gates that form the shape of the dot. Here we briefly discuss quantum pumping (see figure 9) when the dc voltage generated by the pump is measured, similar to the experiment by Switkes *et al* [69]. For slow variations of the shape of the dot, we can use the scattering matrix $\mathcal{S}(\varepsilon)$ and later include Coulomb interactions self-consistently [62, 70]. The Coulomb potential is found from the condition of charge conservation. Using a global gauge transformation, it can be shifted into the phases of the scattering states. However,

such a transformation in itself does not pump electrons. The potential cannot be considered as an additional independent pump parameter similar to $X(t)$.

We consider a two-terminal quantum dot with two weak potentials $X_{1,2}$ varied with the same frequency ω. In order to derive a formula for the dc voltage V, we use a simple model for the quantum dot and the two electron reservoirs; see figure 9(*a*). The dot and reservoirs 1, 2 are connected to a screening gate via capacitances C and $C_{1,2}$. Following [71, 72], we introduce the emissivity $e\partial q(\alpha)/\partial X_j$ and $e\partial q(\alpha)/\partial E$, which is the charge that exits the dot through a point contact α ($\alpha = 1, 2$) when the parameter X or chemical potential E is changed:

$$\frac{\partial q(\alpha)}{\partial X} = \frac{1}{2\pi \mathrm{i}} \operatorname{tr} \mathcal{S}^\dagger \mathbf{1}_\alpha \frac{\partial \mathcal{S}}{\partial X}, \qquad \frac{\partial q(\alpha)}{\partial E} = \frac{1}{2\pi \mathrm{i}} \operatorname{tr} \mathcal{S}^\dagger \mathbf{1}_\alpha \frac{\partial \mathcal{S}}{\partial E}. \tag{32}$$

The total current I_1 flowing through contact 1 is

$$C_1 \frac{\mathrm{d}V_1(t)}{\mathrm{d}t} = I_1(t) = \mathrm{e} \sum_{i=1}^{2} \frac{\partial q(1)}{\partial X_i} \frac{\mathrm{d}X_i}{\mathrm{d}t} + \frac{e^2}{h} g[V_1(t) - V_2(t)], \tag{33}$$

where $g = \operatorname{tr} \mathcal{S}^\dagger \mathbf{1}_1 \mathcal{S} \mathbf{1}_2$ is the conductance of the quantum dot. A similar expression determines I_2. For slow variations of X we can restrict ourselves to first-order time-derivatives only. Since $I_j = C_j \, \mathrm{d}V_j/\mathrm{d}t$, in the limit $\omega \ll G/C_{1,2}$ we have $I_1(t) = \eta I_2(t)$, where $\eta = C_1/C_2$ is a numerical coefficient describing the capacitive division between the two reservoirs. The dc voltage for small periodic parameters with amplitudes $X_{1,2}$ and phase difference $\phi = \phi_1 - \phi_2$ is $\bar{V} = (h\omega/4e) X_1 X_2 \bar{v} \sin\phi$, where [73]

$$\bar{v} = \frac{1}{1+\eta} \left[\frac{\partial}{\partial X_2} \left(\frac{1}{g} \frac{\partial (q(1) - \eta q(2))}{\partial X_1} \right) - \frac{\partial}{\partial X_1} \left(\frac{1}{g} \frac{\partial (q(1) - \eta q(2))}{\partial X_2} \right) \right]. \tag{34}$$

The derivatives with respect to X_1 and X_2 in equation (34) are taken at constant values of the chemical potential E of the reservoirs. However, when the Coulomb interaction is accounted for, it is the sum of chemical potential and local self-consistent Hartree potential U, which is constant. Therefore, in the presence of Coulomb interactions the expressions for the transmitted charge should take this into account [70]. In the limit of weak intra-dot interactions, $e^2/C \ll \Delta$, one still can apply the non-interacting theory and take all derivatives with respect to shape-varying potentials $X_{1,2}$ at fixed value of E. On the other hand, in the strong electron–electron interaction limit, $e^2/C \gg \Delta$, which is usually relevant in experiments, transport occurs on the background of almost constant charge q in the dot. Following Brouwer [62] we can relate derivatives with respect to X at constant E and q and in this way include a Hartree potential of arbitrary strength.

First we note that the applied potentials X, the chemical potential E and the charge of the dot Q are not independent variables. If we denote the derivative of some function F with respect to X at constant Y as $(\partial F/\partial X)_Y$, then

$$\mathrm{d}F(E, Q, X) = \mathrm{d}X \left(\frac{\partial F}{\partial X} \right)_E + \left(\frac{\partial F}{\partial E} \right)_X \left(\mathrm{d}X \left(\frac{\partial E}{\partial X} \right)_q + \mathrm{d}q \left(\frac{\partial q}{\partial E} \right)_X \right), \tag{35}$$

which allows us to write

$$\left(\frac{\partial}{\partial X} \right)_q = \left(\frac{\partial}{\partial X} \right)_E + \left(\frac{\partial E}{\partial X} \right)_q \partial_E = \left(\frac{\partial}{\partial X} \right)_E - \frac{(\partial q/\partial X)_E}{(\partial q/\partial E)_X} \partial_E. \tag{36}$$

The derivatives in the last equation in equation (36) are found as follows: the denominator is evaluated in the absence of pumping (constant X) as a balance of particle current and displacement current from the dot, $\left(\sum_{\alpha\beta} G_{\alpha\beta}(\omega) + \mathrm{i}\omega C\right) \mathrm{d}E = \mathrm{i}\omega e \mathrm{d}q_\omega$, so that the derivative is $\partial q_\omega/\partial E = (C/C_\mu) \operatorname{tr} \mathcal{N}$. The numerator is evaluated at constant E, so the dependence of $\mathcal{S}$ on the pumping parameter X is crucial. Unlike the dc-pumped current, found by Brouwer to

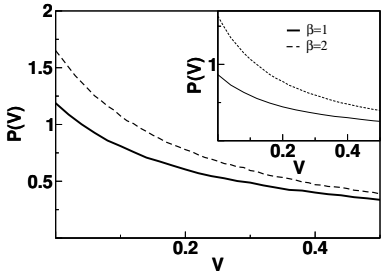

Figure 10. Mesoscopic distribution $P(\bar{v})$ of pumped voltage $\bar{v}$ is presented for $N_1 = N_2 = 1$ with and without time-reversal symmetry (solid and dashed curves respectively). The limits of strong, $C/e^2 \ll \Delta$ (main figure, after [73]), and weak interaction, $C/e^2 \gg \Delta$ (inset), are similar to each other.

be quadratic in pumped strengths [62], the ac-component I_ω is linear in X and can be found by expansion of $\mathcal{S}([X(t)])$ in X to first order. As a result, $\partial q_\omega/\partial X_\omega = \mathrm{tr}\,\mathcal{N}_X$. If analogously to equations (1) and (2) we introduce the matrix $\mathcal{N}_X = (1/2\pi\mathrm{i})\mathcal{S}^\dagger\partial_X\mathcal{S}$ then

$$\frac{\partial E}{\partial X} = -\frac{C_\mu}{C}\frac{\mathrm{tr}\,\mathcal{N}_X}{\mathrm{tr}\,\mathcal{N}}. \tag{37}$$

In the non-interacting limit $C \to \infty$, only the first term in the rhs of equation (36) survives. In the opposite limit $C \to 0$ of a realistic quantum dot the charging energy is large, $e^2/C \gg \Delta$. Then one finds that the charge of an open dot essentially remains constant during the pumping cycle, $I_1(t) = -I_2(t)$ for all time t. As a consequence, the pumped voltage $\bar{v}$ loses its dependence on the capacitive division η, the ratio $C_\mu/C \to 1$ and therefore the derivatives with respect to X are

$$(\partial_X)_q = (\partial_X)_E - \frac{\mathrm{tr}\,\mathcal{N}_X}{\mathrm{tr}\,\mathcal{N}}\partial_E. \tag{38}$$

Using equations (36) and (37) and using the emissivity $\partial q/\partial E$ (32) we reformulate equation (34) for arbitrary interaction. The distribution of $\mathcal{N}_X$ in the numerator of equation (38) is known [18], so that one can perform numerical integration for few-channel dots or use the diagrammatic technique [74] to find the distribution of relevant quantities, e.g. the pumped voltage $\bar{v}$.

The pumped voltage $\bar{v}$ is zero when averaged over an ensemble of dots, and the width of the distribution $P(\bar{v})$ is expected to diminish with growing N, similarly to the distribution $P(\bar{i})$ of the pumped current [62]. Reference [73] finds that in the multi-channel limit the distribution has a Gaussian shape with rms $\langle\bar{v}^2\rangle^{1/2} = (2/\pi N^2)$, since the fluctuations of conductance become small and the conductance takes its classical value, $g = N/2$. However, in the few-channel limit $N_1 = N_2 = 1$ the mesoscopic distribution is wide; see figure 10. The distributions in the limits of weak and strong Coulomb interaction, treated with the help of equation (38), are similar to each other (in the weak interaction limit we take symmetric capacitive division, $\eta = 1$). Particularly, for $\beta = 2$ numerics give almost identical curves. Thus the self-consistent internal potential does not change distributions significantly, a conclusion that, for pumped currents, was reached previously in [62].

8. Shot noise of photon excited electron–hole pairs

In this section, we consider the charge fluctuations and the zero-frequency current noise generated by oscillating potentials applied to the contacts and the gate of a multi-channel

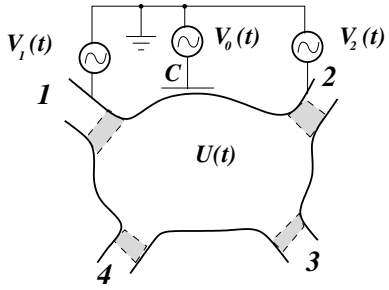

Figure 11. Schematics of a noise measuring set-up. A four-terminal ($M = 4$) chaotic dot is subject to oscillating potentials $V_\alpha(t)$ at contacts $\alpha = 1, 2$ and coupled to a gate with a time-dependent potential $V_0(t)$, via a capacitance C. The internal potential of the dot is $U(t)$. Tunnelling elements (shaded areas) partially close the dot.

chaotic sample with $M \geqslant 4$ leads (see figure 11). Several contacts are subject to periodic ac-potentials $V_\alpha(t) = V_\alpha \cos(\omega t + \phi_\alpha)$ at the same frequency ω but possibly with different phases ϕ_α. We consider the case $eV_\alpha \ll \hbar\omega$, where the amplitude of the applied potentials eV_α is small compared to the modulation quantum $\hbar\omega$. The oscillating potentials excite the electron gas in the contacts by creating electron–hole pairs. These photon-excited carriers are then reflected at the sample or transmitted through the sample into another contact. There is no dc-current linear in voltage.

We find the effect of Coulomb interactions on the noise through such a multi-channel, ac-biased (partially) open quantum dot for arbitrary frequencies ω and interaction strength; see figure 11. Since in an experiment with dots or similar structures [75, 76] frequencies ω might be comparable to the inverse dwell time, one cannot restrict oneself to first energy derivatives only. Consequently, the Wigner–Smith matrix is not as useful for arbitrary ω, since we have to consider correlations of electrons at quite different energies. However, in the limit $N \gg 1$ for open, or high total transmission $\mathrm{tr}\,\hat{\Gamma} \gg 1$ for partially open cavities we can investigate correlations at arbitrary ω.

As emphasized in the introduction, the Coulomb interaction is very important for frequency-dependent transport. In the non-interacting theory, the noise of photon-assisted carriers was discussed by Lesovik and Levitov [77] and Pedersen and Büttiker [78] for energy-independent scattering matrices. This is a good approximation if the frequency ω is sufficiently small, $\omega\tau_\mathrm{d} \ll 1$. The sample-specific results of [77, 78] are in a good agreement with an experiment by Reydellet *et al* [75] in quantum point contacts. However, if an experiment is performed at high frequencies, such that $\omega\tau_\mathrm{d} \sim 1$, the non-interacting theory provides a result which is not gauge invariant [79]. In reality, the frequency dependence should be treated by taking Coulomb interactions into account. In the set-up shown in figure 11, we consider the current correlations in the leads λ, μ using scattering theory for chaotic systems [2, 4].

The rate of photon-generated pairs is small [80]. If the pairs are split into different contacts, they generate current noise. For a single ac-voltage, this noise corresponds to electron–hole correlations of elements of a pair. For several ac-bias voltages, an adjustment of the phase shift between them allows one to maximize (minimize) noise and extract information about the scattering matrix [80]. This is why it is interesting to find current noise correlations $S_{\lambda\mu}$ between λth and μth leads for a multi-lead (partially) open quantum dot. Similar results were obtained by Samuelsson and the authors in [79] for completely open dots.

Below we first discuss shot noise for open quantum dots and show why it is necessary to take the Coulomb interaction into account. Subsequently we discuss the noise correlations

to leading order in $\operatorname{tr}\hat{\Gamma}$ for partially open dots, where the total transparency is still large $\operatorname{tr}\hat{\Gamma} \gg 1$. In this limit, the mesoscopic fluctuations of the noise S can be neglected, so that the result gained from mesoscopic averaging is representative. Corrections to the noise due to the symmetry appear in sub-leading orders, so we do not distinguish here between $\beta = 1, 2$. The coherent open dot with N channels is fully characterized by its $N \times N$ scattering matrix $\mathcal{S}$. Scattering is spin independent and the results given below are presented for a single-spin direction. The dot is assumed fully coherent and the effects of inelastic scattering and dephasing are discussed in [79]. We use units $e = h = k_{\mathrm{B}} = 1$.

We start by expressing the sample-specific noise $S_{\lambda\mu}$ in terms of energy-dependent scattering matrices $\mathcal{S}(\varepsilon)$, amplitudes of applied voltages V_α, their phases ϕ_α and the electron distributions in the leads $f_\alpha(\varepsilon)$. Reference [80] finds

$$S_{\lambda\mu} = \frac{e^2}{2\omega} \operatorname{Re} \sum_{m,\alpha\beta} \operatorname{tr}(\mathbf{A}_{\alpha\beta}(\lambda, m\omega)\mathbf{A}_{\beta\alpha}(\mu, 0)) \left(\delta_{m,0} V_\alpha^2 - V_\alpha V_\beta \delta_{m,1} \, \mathrm{e}^{\mathrm{i}(\phi_\beta - \phi_\alpha)}\right), \tag{39}$$

where $\mathbf{A}(\lambda, \varepsilon) = \mathbf{1}_\lambda - \mathcal{S}^\dagger(\varepsilon)\mathbf{1}_\lambda \mathcal{S}(\varepsilon)$. In the non-interacting low-frequency limit, such that $\mathcal{S}$ is energy-independent, the ensemble averaged noise is [79]

$$S^{\mathrm{o}}_{\lambda\mu} = \frac{2\bar{G}_{\lambda\mu}}{N^2\omega} (N \operatorname{tr} V^2 - |\operatorname{tr} V \, \mathrm{e}^{\mathrm{i}\phi}|^2), \tag{40}$$

where we introduced the averaged conductance of the open quantum dot $\bar{G}_{\lambda\mu} = (N_\lambda \delta_{\lambda\mu} - N_\lambda N_\mu / N)$ and diagonal matrices of the amplitudes $V = \operatorname{diag}(V_1 \mathbf{1}_1, \ldots, V_M \mathbf{1}_M)$ and phase shifts $\phi = \operatorname{diag}(\phi_1 \mathbf{1}_1, \ldots, \phi_M \mathbf{1}_M)$. This result is gauge invariant, that is an arbitrary uniform shift of all Fourier components of potentials $V_{\alpha,\omega} = V_\alpha \exp(\mathrm{i}\phi_\alpha)$ by a potential $U \exp(\mathrm{i}\psi)$ does not have any physical consequence. We note here that although formally the second term in equation (40) is of order $\mathcal{O}(1/N^2)$, the traces in the numerator can be of order N, so that both terms may be of the same order. For example, when a global shift of potentials is applied both terms are equally important.

However, if we are at sufficiently high frequencies, $\omega\tau_{\mathrm{d}} \sim 1$, the energy dependence of $\mathcal{S}$ is important, and the noise spectra are given by

$$S_{\lambda\mu} = S^{\mathrm{o}}_{\lambda\mu} + \frac{2\bar{G}_{\lambda\mu}}{N^2\omega} \frac{|\operatorname{tr} V \, \mathrm{e}^{\mathrm{i}\phi}|^2}{1 + (\omega\tau_{\mathrm{d}})^{-2}}. \tag{41}$$

These spectra are not gauge invariant because of the second term. This is a consequence of the fact that we neglected the internal potential U of the dot and the effect of external gates with potential $V_0 \cos(\omega t + \phi_0)$ capacitively coupled to the dot. Therefore now we consider explicitly the effect of the induced internal potential U_ω. The sample-specific formula (39) for the non-interacting system can be used again if we shift all potentials $V_\omega \to V_\omega - U_\omega$, including unbiased leads.

To proceed we find the *mesoscopically averaged* potential $\bar{U}_\omega$ for a partially open dot. The mesoscopic fluctuations of the potential (9) around the average are small due to the large parameter $\operatorname{tr}\hat{\Gamma} \gg 1$, so we are justified to use $\bar{U}_\omega$ if we are interested in current correlations only to leading order. As a consequence, any effects related to time-reversal symmetry are neglected both in $\bar{U}_\omega$ and, in the end, in the noise $S_{\lambda\mu}$. At high frequencies, $\omega\tau_{\mathrm{d}} \sim 1$, we have to fully account for the frequency dependence of $\bar{U}_\omega$. The leading order of equation (A.4) for the pair correlator of energy-dependent scattering matrices [5, 81] allows us to find the average of the potential U_ω and its derivatives,

$$\bar{U}_\omega = V_0 \, \mathrm{e}^{\mathrm{i}\phi_0} + \frac{C_\mu / C}{1 - \mathrm{i}\omega R C_\mu} \left(\frac{\operatorname{tr} \hat{\Gamma} V \, \mathrm{e}^{\mathrm{i}\phi}}{\operatorname{tr}\hat{\Gamma}} - V_0 \, \mathrm{e}^{\mathrm{i}\phi_0} \right), \qquad \frac{\partial \bar{U}_\omega}{\partial V_{\alpha,\omega}} = \frac{C_\mu / C}{1 - \mathrm{i}\omega R C_\mu} \frac{\operatorname{tr}\hat{\Gamma}_\alpha}{\operatorname{tr}\hat{\Gamma}}, \tag{42}$$

where we introduced $R = 1/\mathrm{tr}\,\Gamma$, which corresponds to the ensemble-averaged charge relaxation resistance $\langle R_q \rangle$ given in equation (13) for a partially open dot; see also equation (16). For an open dot, $\hat{\Gamma} \equiv \mathbf{1}$ the result corresponds to that of [79]. We see that the dwell time $\tau_\mathrm{d} = 1/(\mathrm{tr}\,\hat{\Gamma}\Delta)$ of matrix correlators is replaced by the RC-time of charge relaxation inside the dot, $\tau = \langle C_\mu \rangle R$. This substitution usually occurs in leading order in N. The $\omega \to 0$, $\Gamma = 1$ limit of equation (42) could be easily obtained from equation (10) using the Wigner–Smith matrix and ensemble averaging (using results of [18]). From equation (42) for $\Gamma = 1$ and a shift of all potentials $V_{\omega,\alpha}$ as described above, we obtain with a little algebra [79]:

$$S_{\lambda\mu} = \frac{2\bar{G}_{\lambda\mu}}{N^2\omega}\left(N\,\mathrm{tr}\,V^2 - |\mathrm{tr}\,V\,\mathrm{e}^{\mathrm{i}\phi}|^2 + \frac{|\mathrm{tr}\,V\,\mathrm{e}^{\mathrm{i}\phi} - NV_0\,\mathrm{e}^{\mathrm{i}\phi_0}|^2}{1+(\omega\tau)^{-2}}\right). \tag{43}$$

The second term in this equation is obviously gauge invariant and should be contrasted with that in equation (41). Experimentally, one usually has $\omega\tau \ll 1$ because the Coulomb interaction is sufficiently strong, and the second term in equation (43) vanishes. Thus the non-interacting low-frequency limit (40) is recovered. The fact that the limits of strong interaction at $\omega\tau \ll 1$ and weak interaction at $\omega\tau_\mathrm{d} \ll 1$ provide the same result explains why the results of the non-interacting theories of [77, 78] are in good agreement with experiment [75]. At sufficiently high frequencies, which are in the range of modern experiments, the difference will become apparent.

If one now considers a partially open quantum dot with channel transparencies $\Gamma_i \neq 1$, a similar treatment is possible. For simplicity, we consider the case when all channels have the same transparency $\Gamma_i = \Gamma$. One has to use equation (A.6) for the correlators of scattering matrices. As above, the external gates with potential $V_0(t) = V_0\cos(\omega t + \phi_0)$ are capacitively coupled to the dot via a capacitance C. To demonstrate the gauge-invariance of the final result for the noise, we assume that the current-measuring leads λ, μ are also biased. Then the non-interacting noise is given by an expression analogous to equation (40):

$$\begin{aligned} S^\mathrm{o}_{\lambda\mu}(\Gamma) = {} & \frac{2\Gamma}{N^2\omega}\left(N_\lambda\delta_{\lambda\mu} - \frac{\Gamma N_\lambda N_\mu}{N}\right)(N\,\mathrm{tr}\,V^2 - |\mathrm{tr}\,V\,\mathrm{e}^{\mathrm{i}\phi}|^2) + \frac{\Gamma(1-\Gamma)}{N^2\omega} \\ & \times\left(N_\lambda\delta_{\lambda\mu} - \frac{2N_\lambda N_\mu}{N}\right)(|\mathrm{tr}\,V\,\mathrm{e}^{\mathrm{i}\phi} - NV_\lambda\,\mathrm{e}^{\mathrm{i}\phi_\lambda}|^2 + \ldots|_{\lambda\leftrightarrow\mu}, \end{aligned} \tag{44}$$

where the last term $(\ldots)$ is obtained from the second by swapping $\lambda \leftrightarrow \mu$. If we now take into account the frequency dependence of the scattering matrices similarly to the completely open dot, and use equation (A.6) we find

$$\begin{aligned} S_{\lambda\mu}(\Gamma) = {} & \frac{2\Gamma}{N^2\omega}\left(N_\lambda\delta_{\lambda\mu} - \frac{\Gamma N_\lambda N_\mu}{N}\right)\left(N\,\mathrm{tr}\,V^2 - |\mathrm{tr}\,V\,\mathrm{e}^{\mathrm{i}\phi}|^2 + \frac{|\mathrm{tr}\,V\,\mathrm{e}^{\mathrm{i}\phi} - NV_0\,\mathrm{e}^{\mathrm{i}\phi_0}|^2}{1+(\omega\tau)^{-2}}\right) \\ & + \frac{\Gamma(1-\Gamma)}{N^2\omega}\left(N_\lambda\delta_{\lambda\mu} - \frac{2N_\lambda N_\mu}{N}\right)\left|\frac{\mathrm{tr}\,V\,\mathrm{e}^{\mathrm{i}\phi} - \mathrm{i}\omega\tau NV_0\,\mathrm{e}^{\mathrm{i}\phi_0}}{1-\mathrm{i}\omega\tau} - NV_\lambda\,\mathrm{e}^{\mathrm{i}\phi_\lambda}\right|^2 \\ & + \ldots|_{\lambda\leftrightarrow\mu}. \end{aligned} \tag{45}$$

As an application, consider the cross-correlations in the unbiased leads, $\lambda \neq \mu$ and $V_\lambda = V_\mu = 0$, when $V_0 = 0$:

$$S_{\lambda\mu}(\Gamma) = -\frac{2\Gamma}{N^2\omega}\frac{N_\lambda N_\mu}{N}\left(N\Gamma\,\mathrm{tr}\,V^2 - \frac{3\Gamma-2}{1+\omega^2\tau^2}|\mathrm{tr}\,V\,\mathrm{e}^{\mathrm{i}\phi}|^2\right). \tag{46}$$

Notice that the interactions can not change the negative sign of cross-correlations. For sufficiently transparent barriers, $\Gamma > 2/3$, the Coulomb interactions diminish the absolute

value of the cross-correlation (46). This is easy to see from the dependence of the RC-time on the geometrical capacitance, $\tau^{-1} = \mathrm{tr}\,\hat{\Gamma}(\Delta + e^2/C)$. Indeed, the interactions in the form of the Hartree potential lead to additional (displacement) currents, so that their fluctuations 'damp' particle current fluctuations [79]. On the contrary, for $\Gamma < 2/3$ the 2nd term in equation (46) becomes positive and Coulomb interactions *enhance* the noise. Indeed, for $\Gamma \to 0$ the response of the dot becomes capacitive rather then resistive (see the denominator in equation (42)), and the displacement currents fluctuate out of phase.

Next, similarly to van Langen and Büttiker [82], we consider the exchange correlation $P^{\mathrm{ex}}(\phi)$. This is the difference of the noise S_{34} with bias $V_{1,\omega} = V^*_{2,\omega} = V\,\mathrm{e}^{\mathrm{i}\phi/2}$ and of the sum of the noises for $V_1 = 0$, $V_2 = V$ and $V_1 = V$, $V_2 = 0$. For a four-channel dot, we finds

$$P^{\mathrm{ex}}(\phi) \equiv S_{34}(V\,\mathrm{e}^{\mathrm{i}\phi/2}, V\,\mathrm{e}^{-\mathrm{i}\phi/2}) - S_{34}(V,0) - S_{34}(0,V) = \frac{V^2\cos\phi}{16\omega}\frac{\Gamma(3\Gamma-2)}{1+\omega^2\tau^2}. \tag{47}$$

For a dc-biased dot, the inversion of the sign of the exchange correlation at $\Gamma = 2/3$ was found previously [82]. Note that Coulomb interactions enhance the absolute value of the exchange correlation (47).

9. Discussion of related works

In this section, we briefly allude to alternative approaches to treat the Coulomb interaction and discuss the applicability of the results presented above. In this paper we used the RPA approach to the Coulomb interaction which is built into the scattering matrix approach by Büttiker and co-workers [71, 72, 83, 84]. Another, often favoured, path is the Hamiltonian approach. For non-interacting electrons, it is completely equivalent to the scattering approach [85, 86] and which method one uses is a matter of taste. Aleiner, Brouwer and Glazman [5] demonstrated how the Coulomb interactions can be considered in the Hamiltonian approach. The interaction Hamiltonian has a hierarchical structure: its universal part depends only on the number of electrons inside and the energy-scale e^2/C. The non-universal terms due to non-uniformity of the potential in the dot [5, 87] are small, $\ll\Delta$. Writing the Hamiltonian of the total system as a sum of Hamiltonians of the closed interacting dot, of the leads, and the coupling term, one can express transport quantities and proceed with a Green function formulation [5, 88]. Then the Coulomb potential is usually considered in several theoretical limits: either for arbitrary number of channels N, if the interaction strength is small [89–92], or in a diagrammatic expansion in $1/N \ll 1$ for arbitrary interaction strength [93–96]. One can see that the total transmission $\mathrm{tr}\,\hat{\Gamma}$ is an essential parameter of the problem.

It is known from the literature that the mean-field treatment, which renormalizes the interaction line, cannot lead to such effects as, e.g. charge quantization in blockaded quantum dots [21]. However, in the multi-channel limit $N \gg 1$ the exchange terms can be neglected, and the Hartree potential of the dot provides the leading effect of the Coulomb interaction. Therefore, one expects that in a crossover from multi-channel systems to the Coulomb blockade regime, the exchange contributions may become important. Only very recently did Brouwer, Lamacraft and Flensberg [88] consider a unified approach using a Keldysh technique and scattering matrix theory. They demonstrated that the exchange diagrams may become important when the number of conducting channels N becomes small, and so for the dot with poor transmission a Hartree treatment is not enough. For the variance of the electro-chemical capacitance C_μ and the density of states $\nu(\varepsilon)$, as well as for the variance of the charge pumped by a quantum pump, the corrections due to exchange were found to be $\mathcal{O}(1/N)$ for $N \gg 1$. The self-consistent theory by Büttiker and co-workers is reproduced for open coherent dots to leading order in $1/N$. The inclusion of exchange terms to arbitrary order

is a challenging task, but the authors [88] argue that the expansion in $1/N$ is still useful even for two-channel systems ($N = 4$ if spin degeneracy is taken into account) and the proposed diagrammatic technique in $1/N$ can still be used for few-channel dots. As another example of an application of a $1/N$-expansion to few-channel open dots, we mention the recent work by Vavilov, DiCarlo and Marcus [97]. There the strong Coulomb interaction was treated as a self-averaging Hartree potential and was transformed into the phases of scattering states in the leads. Good agreement with experiment is reported for the variance of the photovoltaic current, if the leading in N term is used when $N = 2$.

To summarize, we expect that the self-consistent treatment of the Coulomb interaction within the scattering approach is still qualitatively correct down to $N = 1 - 2$ channels. Measurement of transport involving sufficiently high frequency ω would clarify the question of the importance of the exchange terms [39, 98].

10. Conclusions

In this work, we have focused on transport problems in which dynamic charge fluctuations play an essential role. Chaotic quantum dots provide an example of a generic conductor which serves to illustrate the basic role which the long-range Coulomb interaction plays in problems of this type. The isotropic chaotic scattering allows us in many cases to treat interaction effects with just a single potential. As a consequence, we can simplify the theoretical discussion to an extent which would be unrealistic and inappropriate for less generic conductors. We have pointed out that at low frequencies the charge fluctuations can be described with the help of a generalized Wigner–Smith matrix in which we replace the energy derivative with a derivative with respect to the local electric potential. Together with a self-consistent treatment of the charge response, this leads to a charge operator, which determines capacitances, kinetic inductances, the weakly nonlinear current voltage characteristics, charge relaxation resistances and the low-frequency noise power of charge fluctuations. We have shown how this approach is applied to specific examples, such as the rate of relaxation and decoherence of a charge qubit near a chaotic cavity, or quantum pumping. We have illustrated how the approach is applied to transport problems in which the frequency is not small, discussing the shot noise of photon-excited electron–hole pairs. The unified description of these problems demonstrates the generality of the approach, and makes it a useful tool for future investigations. On the experimental side, there is an increasing interest to explore dynamic phase-coherent transport. This interest derives not only from the fact that the dynamics of small structures is largely an unexplored area, but also from the desire to use quantum coherent structures to perform useful tasks, such as quantum information processing, and to perform these tasks as fast as possible.

Acknowledgments

We acknowledge stimulating discussions with Piet Brouwer, Leo DiCarlo, Julien Gabelli, Christian Glattli, Michael Moskalets and Eugene Sukhorukov. This work was supported by the Swiss National Science Foundation and Marie Curie RTN on Nanoscale Dynamics and Quantum Coherence.

Appendix. Matrix correlators for energy-dependent matrices with non-ideal leads

In this appendix, we present several correlators of the scattering matrix $\mathcal{S}$ of chaotic partially open quantum dot, when the contacts have transmission $\Gamma_i \leqslant 1, i = 1, \ldots, N$. These

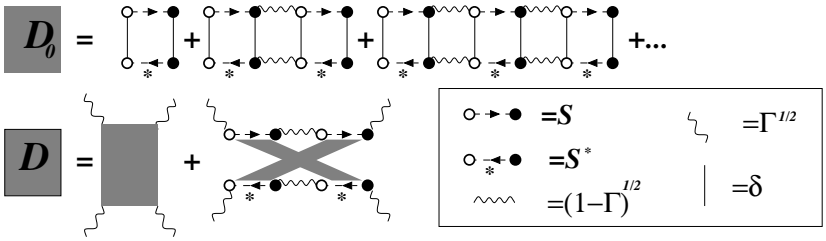

Figure A1. Top: ladder diagrams for the leading order $\mathcal{D}_0$ contribution to full 2-matrix correlator $\mathcal{D} = \langle(\delta\mathcal{S})(\delta\mathcal{S}^*)\rangle$. Bottom: leading and sub-leading terms for $\mathcal{D}$. The second term contributes, e.g., to var G.

correlators are used to find conductance auto-correlations and noise through a biased dot. The imperfect transmission of the contacts is characterized by an $N \times N$ reflection matrix $\bar{\mathcal{S}}$ for which we take the simple form

$$\bar{\mathcal{S}} = \langle\mathcal{S}\rangle = (1 - \hat{\Gamma})^{1/2}, \tag{A.1}$$

where $\hat{\Gamma}$ is an $N \times N$ diagonal matrix containing the transmission coefficients $\Gamma_j \in [0, 1]$. In order to describe coherent energy-dependent scattering with non-ideal leads, we use the following method. An $N \times N$ matrix $\mathcal{U}(\varepsilon)$ of a fully open quantum dot is found using stub model [18, 99, 100]. Energy-independent reflection from the contacts is modelled by $\bar{\mathcal{S}}$, but since the carrier can enter the dot with the probability $\Gamma^{1/2}$, its scattering is described by [86, 101]

$$\mathcal{S}(\varepsilon) \equiv \bar{\mathcal{S}} - \delta\mathcal{S}(\varepsilon) = \bar{\mathcal{S}} - \Gamma^{1/2}\mathcal{U}(\varepsilon)(1 - (1 - \Gamma)^{1/2}\mathcal{U}(\varepsilon))^{-1}\Gamma^{1/2}. \tag{A.2}$$

The matrix correlators below are presented for the case of fully broken time-reversal symmetry, $\beta = 2$. When this symmetry is present, one should add terms which correspond to permutations of indices, so that e.g. for 2-matrix correlator, a Cooperon contribution is added, and for the irreducible four-matrix correlator (Hikami box) each term containing four δ-functions should be supplemented by seven other terms, obtained by permutations of three pairs of indices.

The basic element of diagrammatic technique is a 2-matrix correlator, an ensemble-averaged product of two scattering matrix elements [81]. For convenience we introduce a shorthand notation $D(\varepsilon, \varepsilon') = 1/(\mathrm{tr}\,\hat{\Gamma} - i(\varepsilon - \varepsilon'))$, where $\varepsilon, \varepsilon'$ are normalized by $2\pi/\Delta$. The correlator $\langle\delta\mathcal{S}\delta\mathcal{S}^*\rangle$, shown on figure A1, is

$$\langle(\delta\mathcal{S})_{ij}(\varepsilon)(\delta\mathcal{S})^*_{kl}(\varepsilon')\rangle = \Gamma_i\Gamma_l D(\varepsilon, \varepsilon')(\delta_{ik}\delta_{jl} + \sqrt{(1 - \Gamma_i)(1 - \Gamma_l)}D(\varepsilon, \varepsilon')\delta_{ij}\delta_{kl}). \tag{A.3}$$

Note that the second term is actually sub-leading in $\mathrm{tr}\,\hat{\Gamma}$, but we keep it for reasons to be explained later. Using equation (A.3), we find

$$\begin{aligned}\langle\mathcal{S}_{ij}(\varepsilon)\mathcal{S}^*_{kl}(\varepsilon')\rangle = {} & \sqrt{(1 - \Gamma_i)(1 - \Gamma_l)}\delta_{ij}\delta_{kl} + \Gamma_i\Gamma_l D(\varepsilon, \varepsilon')\delta_{ik}\delta_{jl} \\ & + \sqrt{(1 - \Gamma_i)(1 - \Gamma_l)}\Gamma_i\Gamma_l D^2(\varepsilon, \varepsilon')\delta_{ij}\delta_{kl}.\end{aligned} \tag{A.4}$$

The leading-order term (first line) in equation (A.4) was previously found in [5, 81]. The expressions for correlators of n matrix elements for $n > 2$ are more complicated, and below

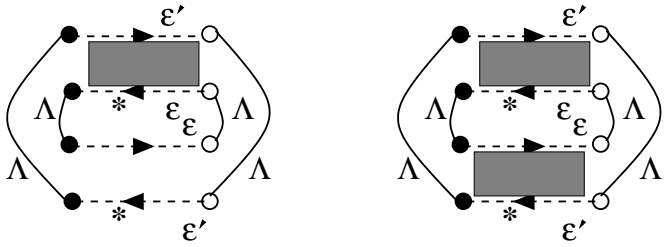

Figure A2. Diagrams for the evaluation of $\langle\langle G(\varepsilon)G(\varepsilon')\rangle\rangle$: (left) a single diffusion $\mathcal{D}$ connects one pair of matrices, the others being averaged to $\langle\mathcal{S}(\mathcal{S}^*)\rangle$; (right) $\mathcal{D}^2$ give diagrams of the same order. For $\beta = 1$ additional contribution comes from the substitution $\mathcal{D} \to \mathcal{C}$ in these diagrams.

we present a 3-matrix correlator of $\delta\mathcal{S}\delta\mathcal{S}^*\delta\mathcal{S}^*$ to a leading order:

$$\langle(\delta\mathcal{S})_{ij}(\varepsilon)(\delta\mathcal{S})^*_{k_1l_1}(\varepsilon_1')(\delta\mathcal{S})^*_{k_2l_2}(\varepsilon_2')\rangle = \Gamma_i\Gamma_j D(\varepsilon,\varepsilon_1')D(\varepsilon,\varepsilon_2') \times \left(\Gamma_j\sqrt{1-\Gamma_j}\delta_{il_2}\delta_{k_2l_1}\delta_{k_1j} + \Gamma_i\sqrt{1-\Gamma_i}\delta_{ik_2}\delta_{l_2k_1}\delta_{l_1j}\right). \tag{A.5}$$

The 4-matrix correlator is equal to the reducible (disconnected) part and the Hikami box denoted by ■ for the irreducible fourth moment:

$$\langle(\delta\mathcal{S})_{i_1j_1}(\varepsilon_1)(\delta\mathcal{S})_{i_2j_2}(\varepsilon_2)(\delta\mathcal{S})^*_{k_1l_1}(\varepsilon_1')(\delta\mathcal{S})^*_{k_2l_2}(\varepsilon_2')\rangle = \blacksquare + \Gamma_{i_1}\Gamma_{i_2}\Gamma_{l_1}\Gamma_{l_2} \times \left(D(\varepsilon_1,\varepsilon_1')D(\varepsilon_2,\varepsilon_2')\delta_{i_1k_1}\delta_{j_1l_1}\delta_{i_2k_2}\delta_{j_2l_2} + D(\varepsilon_1,\varepsilon_2')D(\varepsilon_2,\varepsilon_1')\delta_{i_1k_2}\delta_{j_1l_2}\delta_{i_2k_1}\delta_{j_2l_1}\right), \tag{A.6}$$

$$\begin{aligned}\blacksquare = {}& \Gamma_{i_1}\Gamma_{i_2}\Gamma_{l_1}\Gamma_{l_2}D(\varepsilon_1,\varepsilon_1')D(\varepsilon_2,\varepsilon_2')D(\varepsilon_1,\varepsilon_2')D(\varepsilon_2,\varepsilon_1')\left\{\delta_{i_1k_1}\delta_{j_1l_2}\delta_{i_2k_2}\delta_{j_2l_1}\right.\\ &\times\left([\mathrm{tr}(\Gamma^2-2\Gamma)+\mathrm{i}(\varepsilon_1-\varepsilon_1'+\varepsilon_2-\varepsilon_2')]+\left(1-\Gamma_{i_1}\right)D^{-1}(\varepsilon_1,\varepsilon_1')\right.\\ &+\left(1-\Gamma_{l_2}\right)D^{-1}(\varepsilon_1,\varepsilon_2')+\left(1-\Gamma_{i_2}\right)D^{-1}(\varepsilon_2,\varepsilon_2')+\left.\left(1-\Gamma_{l_1}\right)D^{-1}(\varepsilon_2,\varepsilon_1')\right)\\ &+\delta_{i_1k_2}\delta_{j_1l_1}\delta_{i_2k_1}\delta_{j_2l_2}\left([\mathrm{tr}(\Gamma^2-2\Gamma)+i(\varepsilon_1-\varepsilon_1'+\varepsilon_2-\varepsilon_2')]+\left(1-\Gamma_{i_1}\right)D^{-1}(\varepsilon_1,\varepsilon_2')\right.\\ &+\left(1-\Gamma_{l_1}\right)D^{-1}(\varepsilon_1,\varepsilon_1')+\left(1-\Gamma_{i_2}\right)D^{-1}(\varepsilon_2,\varepsilon_1')+\left.\left(1-\Gamma_{l_2}\right)D^{-1}(\varepsilon_2,\varepsilon_2')\right)\\ &+\left(\delta_{i_1k_1}\delta_{l_1k_2}\delta_{l_2j_2}\delta_{i_2j_1}(1-\Gamma)^{1/2}_{i_2}(1-\Gamma)^{1/2}_{l_1}+\delta_{i_1j_2}\delta_{i_2k_2}\delta_{l_2k_1}\delta_{l_1j_1}(1-\Gamma)^{1/2}_{i_1}(1-\Gamma)^{1/2}_{l_2}\right)\\ &\times[D^{-1}(\varepsilon_1,\varepsilon_1')+D^{-1}(\varepsilon_2,\varepsilon_2')]+\left(\delta_{i_1k_2}\delta_{l_2k_1}\delta_{l_1j_2}\delta_{i_2j_1}(1-\Gamma)^{1/2}_{i_1}(1-\Gamma)^{1/2}_{l_1}\right.\\ &\left.\left.+\delta_{i_1j_2}\delta_{i_2k_1}\delta_{l_1k_2}\delta_{l_2j_1}(1-\Gamma)^{1/2}_{i_2}(1-\Gamma)^{1/2}_{l_2}\right)[D^{-1}(\varepsilon_1,\varepsilon_2')+D^{-1}(\varepsilon_2,\varepsilon_1')]\right\}.\end{aligned} \tag{A.7}$$

We point out that the 4-matrix correlator does not simply reduce N to $\mathrm{tr}\,\hat{\Gamma}$ or $\mathrm{tr}\,\hat{\Gamma}^2$, when the dot becomes partially open. As a result, Hikami box found in appendix A of [81] for partially open dots reproduces equation (A.7) only for $\Gamma = 1$. One can use the correlators (A.4)–(A.7) to find, e.g. the two-terminal dimensionless conductance G through a quantum dot and its correlation function $\langle\langle G(\varepsilon)G(\varepsilon')\rangle\rangle = \langle G(\varepsilon)G(\varepsilon')\rangle - \langle G(\varepsilon)\rangle\langle G(\varepsilon')\rangle$ at different energies. To do this we express conductance in terms of a traceless matrix Λ as

$$G_{12}(\varepsilon) = \mathrm{tr}(\mathcal{S}^\dagger(\varepsilon)\mathbf{1}_1\mathcal{S}(\varepsilon)\mathbf{1}_2) = \frac{N_1N_2}{N} - \mathrm{tr}(\mathcal{S}^\dagger(\varepsilon)\Lambda\mathcal{S}(\varepsilon)\Lambda), \qquad \Lambda \equiv \frac{N_2}{N}\mathbf{1}_1 - \frac{N_1}{N}\mathbf{1}_2. \tag{A.8}$$

Averaging, using 2-matrix correlators, yields the energy-independent conductance:

$$\langle G(\varepsilon)\rangle = \mathrm{tr}\,\hat{\Gamma}\Lambda^2 - \frac{\mathrm{tr}^2\,\hat{\Gamma}\Lambda}{\mathrm{tr}\,\hat{\Gamma}} - \frac{\mathrm{tr}\,\hat{\Gamma}^2\Lambda^2}{\mathrm{tr}\,\hat{\Gamma}}\delta_{\beta,1}. \tag{A.9}$$

To find $\langle\langle G(\varepsilon)G(\varepsilon')\rangle\rangle$ we have to calculate two diagrams shown in figure A2

$$\langle\langle G(\varepsilon)G(\varepsilon')\rangle\rangle = \frac{2}{\beta}\left(2\frac{\mathrm{tr}\,\hat{\Gamma}\,\mathrm{tr}\,\Lambda^4(1-\hat{\Gamma})\hat{\Gamma}^2 + \mathrm{tr}^2\,\Lambda^2(1-\hat{\Gamma})\hat{\Gamma}}{\mathrm{tr}^2\,\hat{\Gamma} + (\varepsilon-\varepsilon')^2} + \frac{\mathrm{tr}^2\,\Lambda^2\hat{\Gamma}^2}{\mathrm{tr}^2\,\hat{\Gamma} + (\varepsilon-\varepsilon')^2}\right). \quad \text{(A.10)}$$

Note that for the left diagram on figure A2, we have to use a sub-leading term from equation (A.3), which gives the $\mathrm{tr}^2\,\Lambda^2(1-\hat{\Gamma})\hat{\Gamma}$ term in equation (A.10). The doubling of the left diagrams comes from possibility of having correlators on the top and bottom. Due to the convenient representation of G in terms of traceless matrix Λ, the irreducible averages (A.5) and (A.7) do not contribute to the correlations. At $\hat{\Gamma} = \Gamma\mathbf{1}$, $N_1 = N_2 = N/2$ and $\varepsilon = \varepsilon'$ we reproduce the result $\mathrm{var}\,G = (2 - 2\Gamma + \Gamma^2)/(8\beta)$ obtained by Brouwer and Beenakker [74], and at $\Gamma = 1$, $\varepsilon \neq \varepsilon'$ we have $\mathrm{var}\,G = (1/8\beta)/(1 + (\varepsilon - \varepsilon')^2/N^2)$ [81, 102, 103].

To obtain equations (43)–(45) we need a correlator (A.6) combined in the form of $\mathbf{A}_{\alpha\beta}(\lambda, \varepsilon)\mathbf{A}_{\beta\alpha}(\mu, \varepsilon')$, the matrices $\mathbf{A}$ are defined after equation (39). One can also use equation (A.6) in the limit $\omega \to 0$ to obtain the noise in a dc-biased dot [82].

References

[1] Sohn L L, Kouwenhoven L P and Schön G (ed) 1997 *Mesoscopic Electron Transport (NATO ASI Series E* vol 345*)* (Dordrecht: Kluwer)
[2] Beenakker C W J 1997 *Rev. Mod. Phys.* **69** 731
[3] Alhassid Y 2000 *Rev. Mod. Phys.* **72** 895
[4] Blanter Ya M and Büttiker M 2000 *Phys. Rep.* **336** 2
[5] Aleiner I L, Brouwer P W and Glazman L I 2002 *Phys. Rep.* **358** 309
[6] Doron E, Smilansky U and Frenkel A 1990 *Phys. Rev. Lett.* **65** 3072
[7] Stein J, Stöckmann H-J and Stoffregen U 1995 *Phys. Rev. Lett.* **75** 53
[8] Verbaarschot J J M, Weidenmüller H A and Zirnbauer M R 1985 *Phys. Rep.* **129** 367
[9] Altshuler B L, Lee P A and Webb R A (ed) 1991 *Mesoscopic Phenomena in Solids (Modern Problems in Condensed Matter Sciences* vol 30*)* (Amsterdam: North-Holland)
[10] Akermans E, Pichard G, Montambaux J-L and Zinn-Justin J (ed) 1994 *Mesoscopic Quantum Physics (Les Houches 1994, Session LXI)* (Amsterdam: Noth-Holland)
[11] Wigner E P 1995 *Phys. Rev.* **98** 145
[12] Smith F T 1996 *Phys. Rev.* **118** 349
[13] Fyodorov Y V and Sommers H J 1996 *Phys. Rev. Lett.* **76** 4709
[14] Gopar V A, Mello P A and Büttiker M 1996 *Phys. Rev. Lett.* **77** 3005
[15] Fyodorov Y V and Sommers H J 1997 *J. Math. Phys.* **38** 1918
[16] Lehmann N *et al* 1995 *Physica* D **86** 572
[17] Brouwer P W, Frahm K M and Beenakker C W J 1997 *Phys. Rev. Lett.* **78** 4737
[18] Brouwer P W, Frahm K M and Beenakker C W J 1999 *Waves Random Media* **9** 91
[19] Büttiker M and Landauer R 1982 *Phys. Rev. Lett.* **49** 1739
[20] Büttiker M 1983 *Phys. Rev.* B **27** 6178
[21] Altshuler B L and Aronov A G 1985 *Electron–Electron Interactions in Disordered Systems* ed A L Efros and M Pollak (Amsterdam: North-Holland) p 1
[22] Blümel R and Smilansky U 1988 *Phys. Rev. Lett.* **60** 477
[23] Baranger H U and Mello P A 1994 *Phys. Rev. Lett* **73** 142
[24] Jalabert R A, Pichard J L and Beenakker C W J 1994 *Europhys. Lett.* **73** 255
[25] Fyodorov Y V, Savin D V and Sommers H J 2005 *Preprint* cond-mat/0507016
[26] Büttiker M, Thomas H and Prêtre A 1993 *Phys. Lett.* A **180** 364
[27] Pedersen M H, van Langen S A and Büttiker M 1998 *Phys. Rev.* B **57** 1838
[28] Leavens C R and Aers G C 1987 *Solid State Commun.* **63** 1107
[29] Büttiker M 1993 *J. Phys.: Condens. Matter* **5** 9361
[30] Büttiker M and Martin A M 2000 *Phys. Rev.* B **61** 2737
[31] Martin A M and Büttiker M 2000 *Phys. Rev. Lett.* **84** 3386
[32] Lambe R and Jacklevic R C 1969 *Phys. Rev. Lett.* **22** 1371
[33] Büttiker M 1987 *Phys. Rev.* B **36** 3548
[34] Luryi S 1988 *Appl. Phys. Lett.* **52** 501

[35] Sánchez D and Büttiker M 2004 *Phys. Rev. Lett.* **93** 106802
[36] Büttiker M 1994 *Phys. Scr.* T **54** 104
[37] Büttiker M and Stafford C A 1996 *Phys. Rev. Lett.* **76** 495
[38] Deblock R *et al* 2000 *Phys. Rev. Lett.* **84** 5379
[39] Gabelli J *et al* 2005 unpublished
[40] Büttiker M 1999 *J. Korean Phys. Soc.* **34** 121
[41] Dyson F J 1962 *J. Math Phys.* **3** 140
[42] Oberholzer S *et al* 2001 *Phys. Rev. Lett.* **86** 2114
[43] Hekking F W J and Pekkola J P 2005 *Preprint* cond-mat/0508450
[44] Nagaev K E, Pilgram S and Büttiker M 2004 *Phys. Rev. Lett.* **92** 176804
[45] Reulet B and Prober D E 2005 *Phys. Rev. Lett.* **95** 066602
[46] Pilgram S and Büttiker M 2002 *Phys. Rev. Lett.* **89** 200401
[47] Buks E *et al* 1998 *Nature* **391** 871
[48] Hayashi T *et al* 2003 *Phys. Rev. Lett.* **91** 226804
[49] Petta J R *et al* 2004 *Phys. Rev. Lett.* **93** 186802
[50] Gurvitz S A 1997 *Phys. Rev.* B **56** 15215
[51] Aleiner I L, Wingreen N S and Meir Y 1997 *Phys. Rev. Lett.* **79** 3740
[52] Levinson Y B 1997 *Europhys. Lett.* **39** 299
[53] Makhlin Y, Schön G and Schnirman A 2001 *Rev. Mod. Phys.* **73** 357
[54] Korotkov A N and Averin D 2001 *Phys. Rev.* B **64** 165310
[55] Clerk A A, Girvin S M and Stone A D 2003 *Phys. Rev.* B **67** 165324
[56] Jordan A N and Büttiker M 2004 *Phys. Rev.* B **71** 125333
[57] Jordan A N and Büttiker M 2005 *Preprint* cond-mat/0505044
[58] Hartmann U and Wilhelm F K 2005 *Preprint* cond-mat/0505132
[59] Averin D V and Sukhorukov E V 2005 *Phys. Rev. Lett.* **95** 126803 (*Preprint* cond-mat/0505647)
[60] Clerk A A 2005 *Preprint* cond-mat/0507223
[61] Spivak B, Zhou F and Beal Monod M T 1995 *Phys. Rev.* B **51** 13226
[62] Brouwer P W 1998 *Phys. Rev.* B **58** 10135
[63] Zhou F, Spivak B and Altshuler B L 1999 *Phys. Rev. Lett.* **82** 608
[64] Shutenko T A, Aleiner I L and Altshuler B L 2000 *Phys. Rev.* B **61** 10366
[65] Avron J E *et al* 2000 *Phys. Rev.* B **62** 10618
[66] Vavilov M G, Ambegaokar V and Aleiner I L 2001 *Phys. Rev.* B **63** 195313
[67] Vavilov M G and Aleiner I L 2001 *Phys. Rev.* B **64** 085115
[68] Moskalets M and Büttiker M 2002 *Phys. Rev.* B **65** 205320
[69] Switkes M *et al* 1999 *Science* **283** 1905
[70] Brouwer P W *et al* 1997 *Phys. Rev. Lett.* **79** 913
[71] Büttiker M, Thomas H and Prêtre A 1994 *Z. Phys.* B **94** 133
[72] Büttiker M, Prêtre A and Thomas H 1993 *Phys. Rev. Lett.* **70** 4114
[73] Polianski M L and Brouwer P W 2001 *Phys. Rev.* B **64** 075304
[74] Brouwer P W and Beenakker C W J 1997 *Phys. Rev.* B **55** 4695
[75] Reydellet L H, Roche P, Glattli D C, Etienne B and Jin Y 2003 *Phys. Rev. Lett.* **90** 176803
[76] DiCarlo L, Marcus C M and Harris J S 2003 *Phys. Rev. Lett.* **91** 246804
[77] Lesovik G B and Levitov L S 1994 *Phys. Rev. Lett.* **72** 538
[78] Pedersen M H and Büttiker M 1998 *Phys. Rev.* B **58** 12993
[79] Polianski M L, Samuelsson P and Büttiker M 2005 *Phys. Rev.* B **72** R161302 (*Preprint* cond-mat/0507336)
[80] Rychkov V, Polianski M L and Büttiker M 2005 *Preprint* cond-mat/0507276
[81] Polianski M L and Brouwer P W 2003 *J. Phys. A: Math. Gen.* **36** 3215
[82] van Langen S A and Büttiker M 1997 *Phys. Rev.* B **56** R1680
[83] Büttiker M and Christen T 1996 *Quantum Transport in Semiconductor Submicron Structures (NATO ASI Ser. E* vol 326*)* ed B Kramer (Dordrecht: Kluwer) p 263
[84] Büttiker M 2000 *J. Low Temp. Phys.* **118** 519
[85] Lewenkopf C H and Weidenmüller H A 1991 *Ann. Phys.* **212** 53
[86] Brouwer P W 1995 *Phys. Rev.* B **51** 16878
[87] Blanter Ya M, Mirlin A D and Muzykantskii B A 1997 *Phys. Rev. Lett.* **78** 2449
[88] Brouwer P W, Lamacraft A and Flensberg K 2005 *Phys. Rev.* B **72** 075316 (*Preprint* cond-mat/0502518)
[89] Flensberg K 1993 *Phys. Rev.* B **48** 11156
[90] Matveev K A 1995 *Phys. Rev.* B **51** 1743
[91] Furusaki A and Matveev K A 1995 *Phys. Rev. Lett.* **75** 709

[92] Furusaki A and Matveev K A 1995 *Phys. Rev.* B **52** 16676
[93] Brouwer P W and Aleiner I L 1999 *Phys. Rev. Lett.* **82** 390
[94] Levy Yeyati A 2001 *Phys. Rev. Lett.* **87** 046802
[95] Golubev D S and Zaikin A D 2001 *Phys. Rev. Lett.* **86** 4887
[96] Golubev D S and Zaikin A D 2004 *Phys. Rev.* B **69** 075318
[97] Vavilov M G, DiCarlo L and Marcus C M 2005 *Phys. Rev.* B **71** R241309
[98] DiCarlo L 2005 Private communication
[99] Brouwer P W and Büttiker M 1997 *Europhys. Lett.* **37** 441
[100] Brouwer P W and Beenakker C W J 1996 *Phys. Rev.* B **54** R12705
[101] Friedman W A and Mello P A 1985 *Ann. Phys.* **161** 276
[102] Efetov K B 1995 *Phys. Rev. Lett.* **74** 2299
[103] Frahm K 1995 *Europhys. Lett.* **30** 457